Renewable and Sustainable Energy Reviews 90 (2018) 453–474

Contents lists available at ScienceDirect

Renewable and Sustainable Energy Reviews

journal homepage: www.elsevier.com/locate/rser

Identification of unknown parameters of solar cell models: A comprehensive overview of available approaches

Rabeh Abbassi[a,b,*], Abdelkader Abbassi[c], Mohamed Jemli[c], Souad Chebbi[a]

[a] University of Tunis, Higher National Engineering School of Tunis (ENSIT), LaTICE Laboratory, 5 Avenue Taha Hussein, PO Box 56, 1008 Tunis, Tunisia
[b] University of Hail, College of Engineering, Saudi Arabia
[c] University of Tunis, Higher National Engineering School of Tunis (ENSIT), Engineering Laboratory of Industrial Systems and Renewable Energies (LISIER), 5 Avenue Taha Hussein, PO Box 56, 1008 Tunis, Tunisia

ARTICLE INFO

Keywords:
Photovoltaic cells
Parameter extraction
I–V and P-V characteristics
Single-diode model
Double-diode model
Three-diode model
Analytical approaches
Numerical approaches

ABSTRACT

Solar energy is increasingly attracting the attention of industry and academia. This heightened focus is mainly motivated by the challenge to contribute to fossil fuels' alternative and to limit the pollution of environment caused by their emissions. The number of researches focusing on solar photovoltaics is continually increasing. The behavior of a photovoltaic (PV) cell/module may be deduced via its current–voltage (I–V) characteristic which depends on its circuit model parameters. Whilst, the extraction of appropriate circuit model DC parameters is crucial to carry out precise performance investigations and control studies on solar PV systems, it remains highly constrained nonlinear non-convex optimization problem. The main objective of this paper is to review the existing research works on PV cell model parameter estimation problem and to assess the performance of the newest approaches. Based on the conducted review of more than 100 methods published over the past 7 years, the recommendations provided for future research are an important goal that will improve the methods of research in this area. In addition, this article implements two real models (single-diode and double-diode) and examines their accuracy to draw the current–voltage (I– V) and power–voltage (P–V) characteristics.

1. Introduction

The share of renewable energies in the world's electricity mix had an exponential growth over the last years (23% in 2015) [1]. This increase, higher than that of conventional energies, will continue over the next four years to reach 28% by 2021. Renewable energies benefit from the dynamic of the Kyoto Protocol, which favors this solution in the fight against greenhouse gases [2,3]. Several technologies, namely wind and solar, have reached a real technical maturity and are now competitive compared to a cost of energy integrating the value of CO_2 [4–8].

Currently, solar energy is more and more becoming as a key element of the future energy mix. It is developing particularly in industrialized countries where the sunshine is favorable and where it is supported by public aid. Regional strategies set important targets for the construction of more than 20 GW of additional CO_2-free [9], in particular solar, electricity production capacity in Mediterranean countries by 2020 [10]. Thus, among the different solar technologies, solar photovoltaic (SPV) represents an important part of the development of renewable energies in the world with rising annual growth rate [11].

The performance of a PV module depends mainly on various factors which include the availability of solar radiation and the efficiency of conversion. Although the average value of conversion efficiency is up to now about 20%, its valuation draws a particular attention from researchers as it can generate optimistic economic predictions that can seduce investor expectations [12]. Indeed, to operate SPV plant at its maximum possible capacity, it is essential to learn about the exact parameters of a solar cell/module [13–15]. However, the conversion efficiency and overall performance of solar cell/module is directly affected by its various physical parameters [16]. Therefore, an accurate estimation of such parameters is always required not only to carry out the evaluation of cell performance but also to improve the design, the optimization of fabricate process and the quality control of the cell [17,18].

According to the majority of the published works [13–19], the I-V and P-V characteristic curves, which derive from the diode model parameters, are very decisive for solar cells/modules being a direct indicator of performance. However, the reverse process of the diode model parameters derivation from the I-V and P-V characteristics remains a key challenge particularly because of the strong nonlinear relationship that governs the PV cell behavior. Various researches [19–21] have been focused on the foremost issues related to the methodologies of the identification of DC solar cell parameters. In [22],

* Corresponding author at: University of Tunis, Higher National Engineering School of Tunis (ENSIT), LaTICE Laboratory, 5 Avenue Taha Hussein, PO Box 56, 1008 Tunis, Tunisia.
E-mail addresses: r_abbassi@yahoo.fr (R. Abbassi), abd_abbassi@yahoo.com (A. Abbassi), mohamed.jemli@isetr.rnu.tn (M. Jemli), chebbi.souad@gmail.com (S. Chebbi).

https://doi.org/10.1016/j.rser.2018.03.011
Received 14 December 2017; Received in revised form 21 February 2018; Accepted 13 March 2018
Available online 24 April 2018
1364-0321/

Nomenclature

DE	Differential Evolution
RADE	Repaired Adaptive Differential Evolution.
PDE	Penalty based DE
IADE	Improved Adaptive DE
AE	Absolute Error
APE	Absolute Power Error
APVE	Absolute Power and Voltage Error
SSE	Sum of Squared Errors
ABCO	Artificial Bee Colony Optimization
AGA	Adaptive Genetic Algorithm
APSO	Particle Swarm Optimization with Adaptive Inertia Weight Control
BBO-M	Bio-Geography Based Optimization with Mutation Strategies
BMO	Bird Mating Optimization
CPSO	Chaos Particle Swarm Optimization
DDM	Double Diode Model
MDDM	Modified Double Diode Model
DEIM	Differential Evolution with Integral Mutation
HS	Harmony Search
IGHS	Improved Global Harmony Search
GGHS	Grouping Based Global Harmony Search
IBCPSO	PSO with Inverse Barrier Constraints
IP	Interior Point
JADE	Adaptive Differential Evolution
LS	Least Square
NR	Newton-Raphson
PSA	Parallel Swarm algorithm
RMSE	Root Mean Squared Error
SBMO	Simplified Bird Mating Optimization
SIV	Suitability Index Variable
GOTLBO	Generalized Oppositional Teaching Based Learning Optimization
STLBO	Simplified Teaching Learning Based Optimization
TVIWAC-PSO	Particle Swarm Optimization with Time Varying Inertia Weight and Acceleration Coefficients
ABSO	Artificial Bee Swarm Optimization
AIS	Artificial Immune System
ANN	Artificial Neural Network
BBO	Bio-Geography Based Optimization
BFA	Bacterial Foraging Algorithm
BPFPA	Bee Pollinated Flower Pollination Algorithm
GA	Genetic Algorithm
IAE	Individual Absolute Error
IGHS	Innovative Global Harmony Search
IPSO	Improved Particle Swarm Optimization
LM	Levenberg-Marquardt
MPCOA	Mutative-Scale Parallel Chaos Optimization
MSE	Mean Squared Error
N.E	Not Extracting
NOCT	Nominal Operating Cell Temperature
PS	Pattern Search
R-JADE	Repaired Adaptive Differential Evolution
SA	Simulated Annealing
SDM	Single Diode Model
ISDM	Improved Single Diode Model
TDM	Three Diode Model-STC: Standard Test Conditions
TLBO	Teaching Learning Based Optimization
VC-PSO	Particle Swarm Optimization with Velocity Clamping
CPU	Central Processing Unit
NMS	Nelder-Mead Algorithm

it has been proved that it is impossible to solve this nonlinear problem accurately relying solely on linear identification methods. Many suggestions [23,24] have been proposed regarding the use of nonlinear electrical models to extract the effective parameters of solar cells accurately and to make sure its operating conditions.

Based on the I-V curves of a P-N junction diode, many models are established to describe the behavior of solar cells. Recently, the literature is richer than previously concerning the estimation of the I-V curves [15,25–33]. The most cited models are the single-diode model (SDM), the double-diode model (DDM), the modified double-diode model (MDDM) and the three-diode model (TDM). Referring to the infinity of published studies, the DDM is judged the almost used for representing the equivalent electrical circuit of solar panel [33–36]. Nonetheless, it has been proven that it is the more complex considering its longer execution time and the nonlinearity relationship of its different parameters [37,38]. On the other side, many researchers have demonstrated that the SDM is the most prevalent taking into account its simplicity [39]. Thus, this model is divided into two different types, which are the Ideal SDM (ISDM) [40] that neglects the series and shunt resistors and the improved SDM that characterizes the relation of its parameters by maintaining the effect of all resistors of the equivalent electrical circuit [41,42]. To extract the parameters of the electrical circuit of solar panel, a multitude of methodologies have been proposed. In this work, these methodologies have been classified into three different families. The first consists in resolving the problem of the nonlinearity of the relation between the different parameters by using mathematical manipulations which are based on the analytical approaches [43–45]. The second family includes essentially the techniques based on the exploitation of several numerical approaches for calculating the parameters of photovoltaic cells [46–49]. These are iterative based algorithms [42].

In addition, metaheuristic approaches are sorted within the third family. These approaches contributed very strongly in the identification of the key parameters of equivalent electrical circuit of PV panels [13,50–52]. In this case, an improved version of modeling based on multitude of algorithms has been used. These techniques are considered as stochastic optimization approaches and has the advantage of being the most effective in term of computational time and accuracy of extracted parameters [38,53–55].

To overcome the drawbacks mentioned in the literature, several methods have been proposed. In this context, this paper aims to exploit this variety of proposed solutions in order to classify and review the existing equivalent electrical circuit, the different parameters extraction techniques and the results found in many previous studies. The advantages and disadvantages of the discussed approaches are summarized and compared according to three different categories. Besides, the most cited types of equivalent electrical circuit has been investigated and implemented carefully. This paper is organized as follows; Section 2 provides an insight into the available electrical circuit models of PV cells. Section 3 reviews, discusses, summarizes and explains the most used techniques of extraction of PV model parameters. In Section 4, the implementation of SDM and DDM models is achieved and the parameters of each of them are extracted. Finally, some conclusions judged very useful for researchers in the field are also drawn by Section 5.

2. Available electrical circuit models of PV cells

2.1. Fundamental

In general, the modeling of a photovoltaic module involves the use of the I-V characteristic of a specific model under well-defined environmental conditions. The design of models that can estimate parameters in a truly representative way remain a complex task [6]. Indeed, the modeling depends on various factors namely the multitude of PV cell types including the number of diodes, shunt resistance (infinite or finite), ideality factor as well as the most appropriate numerical methods [6–49].

According to the literature [13–34], the algorithms for extracting the parameters of the PV cells hinge essentially on the different technologies of the photovoltaic systems, their operating conditions of temperature and illumination and their size. That is why it is extremely important to identify the different parameters that influence the precision of the main equations used for modeling each model [6,55].

Fig. 1 presents five different models of solar cell used in literature. The first one ISDM [18,51,52] is easily understandable but less used (Fig. 1a). The three parameters, which are the short circuit current I_{sc}, the open circuit voltage V_{oc} and the ideality factor A have to be extracted. The second model includes five parameters, which are the short circuit current I_{sc}, the open circuit voltage V_{oc}, the ideality factor A, the series resistance R_s and the shunt resistance R_{sh}. This model has the advantage to be the very accurate model according to the variation of the solar radiation and temperature (Fig. 1b) [15,18,20,22–24,28,30,34–36,38–47,49–53,56]. Fig. 1c shows the DDM model. This model is more complex than that of a single diode, it is characterized by seven key parameters and takes a longer calculation time [13–16,18–20,23,27,28,31–37,48,52,54,55]. The MDDM characterized by eight parameters has also been proposed (Fig. 1d) [25,57]. Besides, a new lumped-parameter equivalent circuit model using three diodes and known as TDM model has been developed (Fig. 1e) [26,58,60].

The current-voltage relation of photovoltaic cell of the ISDM is given by:

$$I = I_{ph} - I_d = I_{ph} - I_0\left(e^{\left(\frac{V+R_sI}{V_t}\right)} - 1\right) \tag{1}$$

In the Eq. (1), the junction thermal voltage at reference conditions is given by:

$$V_t = \frac{AkT}{q} \tag{2}$$

The current-voltage relation of photovoltaic cell of the improved SDM is given by:

$$I = I_{ph} - I_d - I_{sh} = I_{ph} - I_0\left(e^{\left(\frac{V+R_sI}{V_t}\right)} - 1\right) - \frac{V+R_sI}{R_{sh}} \tag{3}$$

The current-voltage relation of photovoltaic cell of the DDM is given by:

$$I = I_{ph} - I_{d1} - I_{d2} - I_{sh} = I_{ph} - I_{01}\left(\exp^{\left(\frac{V+R_sI}{a_1V_{t1}}\right)} - 1\right) - I_{02}\left(\exp^{\left(\frac{V+R_sI}{a_2V_{t2}}\right)} - 1\right) - \frac{V+R_sI}{R_{sh}} \tag{4}$$

The current-voltage relation of photovoltaic cell of the modified double-diode MDDM model is

given by:$$I = I_{ph} - I_{d1} - I_{d2} - I_{sh} = I_{ph} - I_{01}\left(\exp^{\left(\frac{V+R_sI}{a_1V_{t1}}\right)} - 1\right) - I_{02}\left(\exp^{\left(\frac{V+R_sI-I_{d2}R_{s2}}{a_2V_{t2}}\right)} - 1\right) - \frac{V+R_sI}{R_{sh}} \tag{5}$$

The current-voltage relation of photovoltaic cell of the TDM model is given by:

$$I = I_{ph} - I_{d1} - I_{d2} - I_{d3} - I_{sh} = I_{ph} - I_{01}\left(\exp^{\left(\frac{V+R_sI}{a_1V_{t1}}\right)} - 1\right) - I_{02}\left(\exp^{\left(\frac{V+R_sI}{a_2V_{t2}}\right)} - 1\right) - I_{03}\left(\exp^{\left(\frac{V+R_sI}{a_3V_{t3}}\right)} - 1\right) - \frac{V+R_sI}{R_{sh}} \tag{6}$$

Where

I_{ph} is the photocurrent generated at Standard Test Conditions STC (25 °C, 1000 W/m^2) (A)
I_0 is the dark saturation current (A)
q is the electron charge (1.6.10^{-19} C)
T is the cell temperature (K)
R_s is the series resistance (Ω)
R_{sh} is the shunt resistance (Ω).
A is the diode ideality factor
k is the Boltzmann constant (1.38.10^{-23} J/K)

Eqs. (1), (3), (4), (5) and (6) show that the current-voltage relationship of the photovoltaic cell involves various parameters those vary depending on the solar irradiance and cell temperature (n, R_s, R_p,

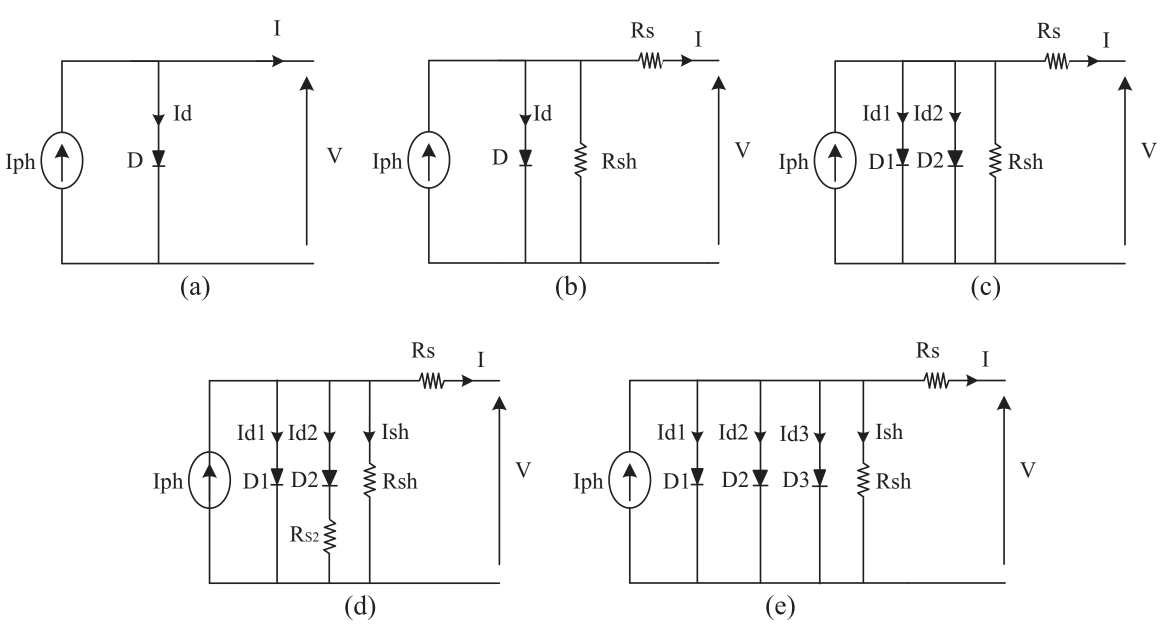

Fig. 1. Equivalent electrical circuit of a solar cell; (a) SDM, (b) ISDM, (c) DDM, (d) MMDM, (e) TDM.

I_o, and I_{ph}). According to literature [10–60], four distinguished models of the photovoltaic cell are commonly used: the ISDM, the SDM, the DDM and the TDM. The expressions (1), (3), (4), (5) and (6) of the characteristic I-V are transcendental equations and can only be solved numerically. However, in order to exploit this characteristic, it is first necessary to determine such parameters. Whatever the model used, the short circuit current and the open circuit voltage are the most important key parameters and without them we cannot do anything. The short circuit current I_{sc} indicates the maximum current that can be delivered by the cell when it is short-circuited, i.e. when the voltage at its terminals is zero. The open-circuit voltage denoted V_{oc}: is that at the terminals of the cell when the cell is in open circuit, that is to say when the current passing through it is then zero. In what follows, we focus on the methods for extracting the parameters of such models of the PV cells.

2.2. Single-diode PV cell model

2.2.1. ISDM parameters extraction

Based on the Eq. (1), the short circuit current (I_{sc}) , the open circuit voltage (V_{oc}), the current (I_m) and the voltage (V_m) at maximum power point (MPP) are given as follows [6,51,52]:

$$I_{sc} = I_{ph}|_{V=0} \tag{7}$$

$$V_{0c} = \frac{nN_sk_BT}{q}\ln\left(1+\frac{I_{sc}}{I_0}\right) \tag{8}$$

$$\exp\left(\frac{qV_{0c}}{nN_sk_BT}\right) = \left(1+\frac{qV_m}{nN_sk_BT}\right)\exp\left(\frac{qV_m}{nN_sk_BT}\right) \tag{9}$$

$$I_m = I_{ph} - I_0\left(\exp\left(\frac{qV_m}{nN_sk_BT}\right)-1\right) \tag{10}$$

At MPP operating point, the derivative of the current with respect to the voltage yields:

$$\frac{dI}{dV} = -\frac{qI_0}{nN_sk_BT}\exp\left(\frac{qV}{nN_sk_BT}\right) \tag{11}$$

At the best operating point of the system (MPP), the corresponding voltage is:

$$V_m = \frac{nN_sk_BT}{q}\ln\left(-\frac{nN_sk_BT}{qI_0}\left(\frac{dI}{dV}\right)_{V_m}\right) \tag{12}$$

Considering the asymptotic behavior describing how the current-voltage curve behaves near the limits of short and open circuit conditions, the derivative appearing in (12) can be evaluated by:

$$\left.\frac{dI}{dV}\right|_{V_m} \cong -\frac{0-I_{sc}}{V_{0c}-0} = -\frac{I_{sc}}{V_{0c}} \tag{13}$$

The current and the voltage at the maximum power point are then determined by substituting the derivative (13) in (11) and (12).

$$V_m = \frac{nN_sk_BT}{q}\ln\left(\frac{nN_sk_BT}{qI_0}\frac{I_{sc}}{V_{0c}}\right) \tag{14}$$

$$I_m = I_{ph} + I_0 - \frac{nN_sk_BT}{q}\left(\frac{I_{sc}}{V_{0c}}\right) \tag{15}$$

Finally, the maximum output power is:

$$P_m = \left(I_{ph} + I_0 - \frac{nN_sk_BT}{q}\left(\frac{I_{sc}}{V_{0c}}\right)\right)\frac{nN_sk_BT}{q}\ln\left(\frac{nN_sk_BT}{qI_0}\frac{I_{sc}}{V_{0c}}\right) \tag{16}$$

Real conditions: taken account the temperature and the solar radiation variation

The majority of PV manufacturers provide the data sheet illustrating only the I-V and P-V curves under standard test conditions (STC). For different temperature or radiation levels it is absolutely necessary to recalculate the critical parameters. The photocurrent is given by the following expression:

$$I_{ph} = (E/E_{ref})(I_{phref} + \mu_i(T-T_{ref})) \tag{17}$$

where

T_{ref}, E_{ref} are respectively the temperature and irradiance at STC conditions, I_{phref} is the reference photocurrent at STC and μ_i is the temperature coefficient of the short circuit current (A/°C). The saturation current is expressed as:

$$I_0 = \frac{I_{scref} + \mu_i(T-T_{STC})}{\exp\left(q\frac{V_{0cref}+\mu_v(T-T_{ref})}{nN_sk_BT}\right)-1} \tag{18}$$

Where

V_{0cref} is the reference open circuit voltage and μ_v is the temperature coefficient of open circuit voltage (V/°C).

Using the maximum power point current (Eq. (10)) and the saturation current at the reference temperature given by Eq. (18), the diode quality coefficient is determined as:

$$N = \frac{q(V_{mref} - V_{0cref})}{N_sk_BT_{ref}}\frac{1}{\ln\left(1-\frac{I_{mref}}{I_{scref}}\right)} \tag{19}$$

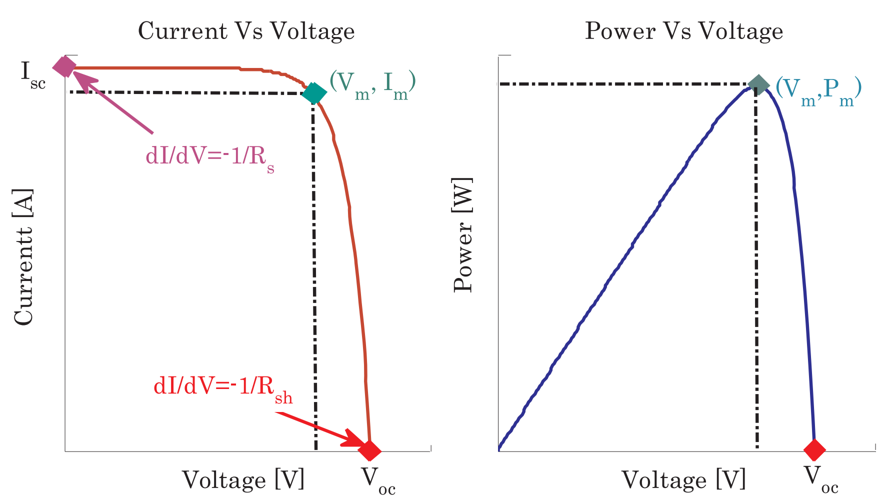

Fig. 2. I-V and P-V characteristics.

Herein, V_{mref}, I_{mref}, V_{Ocref} and I_{Ocref} are provided by manufacturers.

2.2.2. SDM parameters extraction

Under Standard Test Conditions

In STC conditions, the current-voltage relationship that is subject to the Eq. (1) can be rewritten in the following form [28–30]:

$$I = I_{phref} - I_{0ref}\left(e^{\left(\frac{V+R_{sref}I}{V_{tref}}\right)}-1\right) - \frac{V+R_{sref}I}{R_{shref}} \tag{20}$$

where

I_{phref}, I_{Oref}, V_{tref}, R_{sref} and R_{shref} are evaluated in a particular point of current-voltage characteristics curve represented in Fig. 2. The evaluation of the currents of the three critical operating points (short circuit, open circuit and maximum power) makes it possible to establish the relations (21), (22) and (23), respectively.

$$I_{scref} = I_{phref} - I_{0ref}\left(e^{\left(\frac{R_{sref}I_{scref}}{V_{tref}}\right)}-1\right) - R_{sref}\frac{I_{scref}}{R_{shref}} \tag{21}$$

$$I_{phref} - I_{0ref}\left(e^{\left(\frac{V_{0ref}}{V_{tref}}\right)}-1\right) - \frac{V_{0ref}}{R_{shref}} = 0 \tag{22}$$

$$I_{mref} = I_{phref} - I_{0ref}\left(e^{\left(\frac{V_{mref}+R_{sref}I_{mref}}{V_{tref}}\right)}-1\right) - \frac{V_{mref} + R_{sref}I_{mref}}{Rshref} \tag{23}$$

Under standard test conditions, the derivative of the current (3) with respect to the voltage at the open circuit condition and with respect to the short circuit current at the short circuit condition leads to the series resistance R_{sref} and shunt resistance R_{shref}, respectively:

$$\left.\frac{dI}{dV}\right|_{I=0/V=V_{0cref}} = -\frac{1}{R_{sref}} \tag{24}$$

$$\left.\frac{dI}{dV}\right|_{I=I_{scref}/V=0} = -\frac{1}{R_{shref}} \tag{25}$$

The junction thermal voltage at reference conditions is given by:

$$V_{tref} = \frac{AkT_{ref}}{q} \tag{26}$$

Where

I_{scref} is the short circuit current at STC
V_{Oref} is the open circuit voltage at STC
V_{mref} is the voltage at the maximum power point MPP at STC
I_{mref} is the voltage at the maximum power point MPP at STC

The above parameters are normally provided by the manufacturer's datasheet. At MPP, the derivative of the power with respect to the voltage is equal to zero (27):

$$\left.\frac{dP}{dV}\right|_{I=I_{mref}/V=V_{mref}} = 0 \tag{27}$$

From Eqs. (21) and (22), the generated photocurrent I_{phref} and the dark saturation current I_O

can be related by (28):

$$I_{phref} = I_{0ref}\left(e^{\left(\frac{V_{0ref}}{V_{tref}}\right)}-1\right) - \frac{V_{0ref}}{R_{shref}} \tag{28}$$

The substitution of the previous expression into the Eq. (21) gives the relation (29) which can be simplified as (30):

$$I_{scref} = I_{0ref}\left(e^{\left(\frac{V_{0ref}}{V_{tref}}\right)} - e^{\left(\frac{R_{sref}I_{scref}}{V_{tref}}\right)}\right) + \frac{V_{0ref} - I_{scref}R_{sref}}{R_{shref}} \tag{29}$$

$$I_{scref} = I_{0ref}\left(e^{\left(\frac{V_{0ref}}{V_{tref}}\right)}\right) + \frac{V_{0ref} - I_{scref}R_{sref}}{R_{shref}} \tag{30}$$

For I_{Oref}, we will find:

$$I_{0ref} = (I_{scref} \quad - \frac{V_{0ref} - I_{scref}R_{sref}}{R_{shref}})e^{\left(-\frac{V_{0ref}}{V_{tref}}\right)} \tag{31}$$

The substitution of relations (31) and (28) into (23) gives:

$$I_{mref} = I_{0ref} - \frac{V_{mref} + R_{sref}I_{mref} - R_{sref}I_{scref}}{Rshref} - (I_{0ref} - \frac{V_{0ref} - R_{sref}I_{scref}}{R_{shref}})e^{\left(\frac{V_{mref}+R_{sref}I_{mref}}{V_{tref}}\right)} \tag{32}$$

Eq. (27) becomes:

$$\left.\frac{dP}{dV}\right|_{I=I_{mref}/V=V_{mref}} = \frac{d(IV)}{dV} = I+\frac{dI}{dV}V \tag{33}$$

From Eq. (32), the term $\frac{dI}{dV}$ can be given by:

$$\frac{dI}{dV} = \frac{\frac{\partial f(I,V)}{\partial V}}{1-\frac{\partial f(I,V)}{\partial I}} \tag{34}$$

From (34), the Eq. (33) is rewritten as:

$$\left.\frac{dP}{dV}\right|_{I=I_{mref}/V=V_{mref}} = \frac{d(IV)}{dV} = I_{mref} + \frac{\frac{\partial f(I,V)}{\partial V}}{1-\frac{\partial f(I,V)}{\partial I}}V_{mref} \tag{35}$$

Finally, we obtain the following equation:

$$\left.\frac{dP}{dV}\right|_{I=I_{mref}/V=V_{mref}} = I_{mref} + V_{mref}\frac{\frac{-(I_{0ref} - \frac{V_{0ref} - R_{sref}I_{scref}}{R_{shref}})e^{\left(\frac{V_{mref}+R_{sref}I_{mref}}{V_{tref}}\right)}}{V_{tref}R_{shref}} - \frac{1}{R_{shref}}}{1+\frac{(I_{0ref} - \frac{V_{0ref} - R_{sref}I_{scref}}{R_{shref}})e^{\left(\frac{V_{mref}+R_{sref}I_{mref}}{V_{tref}}\right)}}{V_{tref}R_{shref}} - \frac{R_s}{R_{shref}}} \tag{36}$$

Taking into account the Eqs. (25), (35) and (36), the three unknowns R_s, R_{sh} and A_{ref} can be easily found.

$$-\frac{1}{R_{shref}} = \frac{\frac{-(I_{0ref} - \frac{V_{0ref} - R_{sref}I_{scref}}{R_{shref}})e^{\left(\frac{V_{mref}+R_{sref}I_{mref}}{V_{tref}}\right)}}{V_{tref}R_{shref}} - \frac{1}{R_{shref}}}{1+\frac{(I_{0ref} - \frac{V_{0ref} - R_{sref}I_{scref}}{R_{shref}})e^{\left(\frac{V_{mref}+R_{sref}I_{mref}}{V_{tref}}\right)}}{V_{tref}R_{shref}} - \frac{R_s}{R_{shref}}} \tag{37}$$

Based on the relations (32), (36), (37), (28) and (31), the five unknown parameters of SDM model (I_{phref}, I_{Oref}, R_{sref}, R_{shref} and A_{ref}) are easily determined.

Under real conditions: variation of temperature and irradiation

The parameters of the PV module are sensitive to the weather conditions changes as follows. The ideality factor, the saturation current of the diode, the photo-current are given by (38), (39) and (40), respectively:

$$A = A_{ref}(T/T_{ref}) \tag{38}$$

$$I_0 = I_{0ref}(T/T_{ref})^3 e^{\left(\frac{E_g N_s}{V_{tref}\left(1-\frac{T_{ref}}{T}\right)}\right)} \tag{39}$$

$$I_{ph} = (G/G_{ref})(I_{phref} + \alpha_{Isc}(T-T_{ref})) \tag{40}$$

Herein, T, T_{ref}, G and G_{ref} are the cell junction ambient and reference temperatures, instantaneous solar irradiances and instantaneous solar irradiance and standard test conditions irradiance, respectively. $E_g$is the band gap energy of semi-conductor. α_{Isc} is the temperature coefficient of short circuit current (A/°C). The open circuit voltage V_{Oc} is:

$$V_{0c} = V_{0cref} - \beta(T_{ref} - T) + V_t \ln(G/G_{ref}) \quad (41)$$

The series resistance, the shunt resistance, the short circuit current, the maximum power point current and the maximum power point voltage are expressed by (42), (43), (44), (45) and (46), respectively:

$$R_s = R_{sref} - \left[\left(\frac{V_t}{I_0}\right)e^{(-V_{0c}/V_t)}\right] \quad (42)$$

$$R_{sh} = R_{shref}(G_{ref}/G) \quad (43)$$

$$I_{sc} = I_{scref}(G/G_{ref}) + \alpha I_{sc}(T - T_{ref}) \quad (44)$$

$$I_m = I_{mref}(G/G_{ref}) \quad (45)$$

$$V_m = V_{mref} - \beta(T_{ref} - T) \quad (46)$$

2.3. DDM parameters extraction

According to the Fig. 1(c), the output current related to the voltage to describe the I-V characteristics of a DDM of solar cells is defined by [13–16]:

$$I = I_{ph} - I_{D1} - I_{D2} - I_{sh} = I_{ph} - I_{01}\left(\exp\left(\frac{V+R_sI}{a_1V_{t1}}\right) - 1\right) - I_{02}\left(\exp\left(\frac{V+R_sI}{a_2V_{t2}}\right) - 1\right) - \frac{V+R_sI}{R_{sh}} \quad (47)$$

where

I_{ph} is the photo current generated by the incident light
I_{01} is the saturation current due to diffusion mechanism
I_{02} is the saturation current because of carrier recombination in space charge region
a_1 is the diode ideality factor for diffusion current
a_2 is the diode ideality factor for generation recombination current
V_{t1} and V_{t2} are the thermal voltages expressed by:

$$V_{t1} = V_{t2} = V_t = \frac{N_skT}{q} \quad (48)$$

Where

N_s is the number of series connected PV cells in the PV panel
K is the Boltzmann's constant (1.38×10^{-23} J/k)

Eq. (47) is composed by seven unknown parameters to be determined, which are I_{ph}, I_{01}, I_{02}, a_1, a_2, R_s and R_{sh}. These parameters are based on the datasheets of the PV module. Manufacturer gives the different parameters at Standard Test Conditions (STC) (1000 W/m^2, 25 °C). However, these data are not available provided that there is variations of solar irradiance and temperature. For this reason, we try to find these parameters in all possible conditions.

Three characteristics points are given by the manufacturer: the open circuit voltage (V_{Oc}, 0), the short circuit current (0, I_{sc}) and the current and voltage at maximum power point MPP (V_{mp}, I_{mp}). Eq. (47) is evaluated at the three characteristics conditions as follows [33–37]:

At the short circuit point:

$$I_{sc} = I_{ph} - I_{01}\left(\exp\left(\frac{R_sI_{sc}}{a_1V_{t1}}\right) - 1\right) - I_{02}\left(\exp\left(\frac{R_sI_{sc}}{a_2V_{t2}}\right) - 1\right) - \frac{R_sI_{sc}}{R_{sh}} \quad (49)$$

At the open circuit point:

$$0 = I_{ph} - I_{01}\left(\exp\left(\frac{V_{0c}}{a_1V_{t1}}\right) - 1\right) - I_{02}\left(\exp\left(\frac{V_{0c}}{a_2V_{t2}}\right) - 1\right) - \frac{V_{0c}}{R_{sh}} \quad (50)$$

At the maximum power point:

$$I_{mp} = I_{ph} - I_{01}\left(\exp\left(\frac{V_{mp}+R_sI_{mp}}{a_1V_{t1}}\right) - 1\right) - I_{02}\left(\exp\left(\frac{V_{mp}+R_sI_{mp}}{a_2V_{t2}}\right) - 1\right) - \frac{V_{mp} + R_sI_{mp}}{R_{sh}} \quad (51)$$

The power supplied by the PV module is obtained by:

$$P = I \times V \quad (52)$$

Eq. (52) is differentiated with respect to Vas follows:

$$\frac{dP}{dV} = \left(\frac{dI}{dV}\right) \times V + I \quad (53)$$

The derivative of the power with respect to the voltage at the maximum power point is zero, thus:

$$\frac{dI}{dV} = -\frac{I_m}{V_m} \quad (54)$$

So, the derivative of (47) with respect to the voltage is given by:

$$\frac{dI}{dV} = -\frac{I_{01}}{a_1V_{t1}}\left(1+R_s\frac{dI}{dV}\right)\exp\left(\frac{V+R_sI}{a_1V_{t1}}\right) - \frac{I_{02}}{a_1V_{t1}}\left(1+R_s\frac{dI}{dV}\right)\exp\left(\frac{V+R_sI}{a_2V_{t1}}\right) - \frac{1}{R_{sh}}\left(1+R_s\frac{dI}{dV}\right) \quad (55)$$

By substituting (55) in (54), we have:

$$\frac{I_m}{V_m} = \frac{I_{01}}{a_1V_{t1}}\left(1+R_s\frac{dI}{dV}\right)\exp\left(\frac{V+R_sI}{a_1V_{t1}}\right) + \frac{I_{02}}{a_1V_{t1}}\left(1+R_s\frac{dI}{dV}\right)\exp\left(\frac{V+R_sI}{a_2V_{t1}}\right) + \frac{1}{R_{sh}}\left(1+R_s\frac{dI}{dV}\right) \quad (56)$$

Using (50), we obtain:

$$I_{ph} = I_{01}\left(\exp\left(\frac{V_{0c}}{a_1V_{t1}}\right) - 1\right) + I_{02}\left(\exp\left(\frac{V_{0c}}{a_2V_{t2}}\right) - 1\right) + \frac{V_{0c}}{R_{sh}} \quad (57)$$

Substituting (57) into (49),

$$I_{sc} = I_{01}\left(\exp\left(\frac{V_{0c}}{a_1V_{t1}}\right) - \exp\left(\frac{R_sI_{sc}}{a_1V_{t1}}\right)\right) + I_{02}\left(\exp\left(\frac{V_{0c}}{a_2V_{t2}}\right) - \exp^{\left(\frac{R_sI_{sc}}{a_2V_{t2}}\right)}\right) + \frac{V_{0c} - R_sI_{sc}}{R_{sh}} \quad (58)$$

Substituting (57) into (51),

$$I_{mp} = I_{01}\left(\exp\left(\frac{V_{0c}}{a_1V_{t1}}\right) - \exp^{\left(\frac{V_{mp}+R_sI_{mp}}{a_1V_{t1}}\right)}\right) + I_{02}\left(\exp\left(\frac{V_{0c}}{a_1V_{t1}}\right) - \exp^{\left(\frac{V_{mp}+R_sI_{mp}}{a_2V_{t2}}\right)}\right) + \frac{V_{0c} - V_{mp}}{R_{sh}} - \frac{R_sI_{mp}}{R_{sh}} \quad (59)$$

$$I_{mp}\left(1+\frac{R_s}{R_{sh}}\right) = I_{01}\left(\exp\left(\frac{V_{0c}}{a_1V_{t1}}\right) - \exp^{\left(\frac{V_{mp}+R_sI_{mp}}{a_1V_{t1}}\right)}\right) + I_{02}\left(\exp\left(\frac{V_{0c}}{a_1V_{t1}}\right) - \exp^{\left(\frac{V_{mp}+R_sI_{mp}}{a_2V_{t2}}\right)}\right) + \frac{V_{0c} - V_{mp}}{R_{sh}} \quad (60)$$

Eqs. (56), (58) and (60) are three independent equations with four unknown variables I_{01}, I_{02}, R_s and R_{sh}.

The derivative of the current with respect to the voltage at the short circuit current is equal to:

$$\left.\frac{dI}{dV}\right|_{\substack{V=0 \\ I=Isc}} = -\frac{1}{R_{sh}} \quad (61)$$

The derivative of the current with respect to the voltage at the open circuit voltage is equal to:

$$\left.\frac{dI}{dV}\right|_{\substack{V=0\\ I=Isc}} = -\frac{1}{R_s} \tag{62}$$

R_{sh} and R_s can be calculated simultaneously by iteratively increasing the value of R_s while simultaneously calculating the R_{sh} value. From Eq. (29) at maximum power point condition, the expression for R_{sh} can be rearranged and rewritten as [33,52]:

$$R_p = \frac{V_{mp} + I_{mp}R_s}{I_{ph} - I_0\left(\exp\left(\frac{V_{mp}+R_sI_{mp}}{a_1V_{t1}}\right) + \exp\left(\frac{V_{mp}+R_sI_{mp}}{a_2V_{t2}}\right)+2\right) - \frac{P_{mp,E}}{V_{mp}}} \tag{63}$$

Where

$P_{mp,E}$ is the maximum power provided by the manufacturer's datasheet.

The initial conditions for both resistances are given by:

$$R_{s0} = 0,\ R_{p0} = \frac{V_{mp}}{I_{scSTC} - V_{mp}} - \frac{V_{0c\_STC} - V_{mp}}{I_{mp}} \tag{64}$$

Now, after defining all the equations governing the current-voltage characteristics of a solar cell, the Eq. (47) is defined in a non-linear manner and it is needed to solve it to check the current-voltage and power-voltage dependence.

Under real conditions: taking into account the variation of the temperature and the solar radiation

The photo-current is given by:

$$I_{ph} = (I_{ph-STC} + K_i(T-T_{STC}))\frac{G}{G_{STC}} \tag{65}$$

Where

$$I_{ph-STC} = I_{sc-STC}\frac{R_p + R_s}{R_p} \tag{66}$$

K_i is temperature coefficient of short circuit current (A/°C)

I_{sc_STC} is the short circuit current at Standard Test Conditions (A)

Taking account the dependency on temperature variation of open circuit voltage and of short circuit current. The reverse saturation current of the diodes D_1 and D_2 can be expressed by the following Eqs. [18,31]:

$$I_0 = I_{01} = I_{02} = \frac{I_{sc-STC} + K_i(T-T_{STC})}{\exp\left(\frac{V_{0c-STC} + K_v(T-T_{STC})}{aV_t}\right)-1} \tag{67}$$

Where

V_{0c_STC} is the open circuit voltage at Standard Test Conditions (V)

K_v is temperature coefficient of open circuit voltage (V/°C)

The integration of the solar variation on the open circuit voltage into Eq. (51), has allowed us to describe this equation in the form [18,48]:

$$I_0 = I_{01} = I_{02} = \frac{I_{sc-STC} + K_i(T-T_{STC})}{\exp\left(\frac{(V_{0c-STC} + K_v(T-T_{STC})) + aV_t\ln\left(\frac{G}{G_{STC}}\right)}{aV_t}\right)-1} \tag{68}$$

$$I_{sc}(G,T) = I_{sc\_STC}\frac{G}{G_{STC}} + K_i(T-T_{STC}) \tag{69}$$

$$V_{0c}(G,T) = V_{0c\_STC} - K_v(T-T_{STC})\frac{G}{G_{STC}} + aV_t\ln\left(\frac{G}{G_{STC}}\right) \tag{70}$$

$$I_{mp}(G,T) = I_{mp\_STC}\frac{G}{G_{STC}} \tag{71}$$

$$V_{mp}(G,T) = V_{mp\_STC}\frac{G}{G_{STC}} - K_v(T-T_{STC}) \tag{72}$$

2.4. MDDM model parameters extraction

In the MDDM, the influence of grain boundary region is taken into consideration. Therefore, an additional resistance R_{S2} is added in series with the second diode D_2 as shown in Fig. 1d. This fact is well justified as the resistivity in the vicinity of grain boundaries is higher than that within the crystallites [25,57]. By applying KCL, the relationship between the supplied current and the voltage is expressed by Eq. (73).

$$I = I_{ph} - I_{d1} - I_{d2} - I_{sh} = I_{ph} - I_{01}\left(\exp\left(\frac{V+R_sI}{a_1V_{t1}}\right)-1\right) - I_{02}\left(\exp\left(\frac{V+R_sI-I_{d2}R_{S2}}{a_2V_{t2}}\right)-1\right) - \frac{V+R_sI}{R_{sh}} \tag{73}$$

2.5. TDM model parameters extraction

Although the ideal values of n_1 and n_2 of TDM were evaluated by 1 and 2 respectively, these values are not valid for industrialized panels of larger size. In addition, the announced values show that the model has two diodes represents deficiencies to correctly represent the different parameters of the solar cells [58].

In [59], it has been proved by simulations and experimental tests made on crystalline Si solar cells that the diode ideality factor, n, increases with increasing defect density. Given the fact that solar cells are vulnerable to increased localized defects during their fabrication, an increase in Donor-Acceptor Pairs (DAPs) that are effective for increasing the recombination rate leads to higher values of the ideality factor n which can reach a value of 5. For this reason, new works have proposed a circuit model equivalent to three diodes that takes into account the leakage current in the periphery [58].

$$I = I_{ph} - I_{01}\{exp\frac{q(V+IR_{s0}(1+KI))}{n_1kT}\} = \frac{I_{sc-STC} + K_i(T-T_{STC})}{\exp\left(\frac{(V_{0c-STC} + K_v(T-T_{STC})) + aV_t\ln\left(\frac{G}{G_{STC}}\right)}{aV_t}\right)-1} \tag{74}$$

In this case study, the series resistance R_s is not assumed to be constant. Therefore, it is evolved as a variable parameter which strictly depends on the load current variation. This variable résistance is indeed replaced with $R_{s0}(1 + KI)$, where I is the load current and k is another parameter [58]. The current through the PV cell for TDM considering the series resistance can be defined by:

$$I = I_{ph} - I_{01}\left\{exp\frac{q(V+IR_{s0}(1+KI))}{n_1kT}-1\right\} - I_{02}\left\{exp\frac{q(V+IR_{s0}(1+KI))}{n_2kT}-1\right\} - I_{03}\left\{exp\frac{q(V+IR_{s0}(1+KI))}{n_3kT}- \quad 1\right\} - \frac{(V+IR_{s0}(1+KI))}{R_{sh}} = I(V, I, \text{parameters}) \tag{75}$$

Where

$$\text{parameters} = (I_{ph}, I_{01}, n_1, I_{02}, n_2, I_{03}, n_3, R_{s0}, \quad K, R_{sh}) \tag{76}$$

3. Extraction of parameters for PV model

3.1. Problem statement

With the potential interest of photovoltaic electricity in scientific and economic terms, photovoltaic cells are being at the heart of the electricity production chain. Competition over optimizing and increasing the efficiency of photovoltaic cells, leads researchers and industrialists to find efficient and reliable methods to determine the intrinsic parameters of these cells [39,61–64]. In the literature several methods have been proposed for the extraction of the parameters of the solar cell models. Two types of approaches have been used: analytical or traditional approaches [18,20,43,45] and numerical or evolutionary approaches [19,28,29,42,51,65]. Each of these methods has drawbacks, either at the level of the complexity of the use and the precision, or at the level of the convergence and the speed. To deal with this challenge in this area, this paper reviews the methods of estimating electrical parameters for SDM, DDM, MDDM and TDM models.

3.2. Overall review on methods of PV cells parameter estimation

In the literature, the SDM is the most used compared with different other models [15,36,38,39,42,47,50–53,61,63,64,66–93]. In all these cases, the evolutionary algorithms are more investigated in comparison with the analytical and the numerical approaches. Among these algorithms, we can cite, in particular, the Genetic Algorithm (GA) [13,61], the Particle Swarm Optimization (PSO) [13,14,61,65,75,77] and the Differential Evolution (DE) [13,33,51,56,61,68,74,78]. In the previous works, the parameters to be extracted varied from 3 to 7 for the SDM and from 4 to 8 for the DDM. Furthermore, 10 parameters have to be extracted for the TDM. This means that the problem reformulation depends entirely on the number of used diodes to describe the equivalent electrical circuit of the solar cell model. For that purpose, a multitude of photovoltaic cell technologies has been investigated like Poly-crystalline, Mono-crystalline, and Thin-film/Amorphous. While, each of them is characterized by its typical performance, influence of temperature, advantages and disadvantages.

The most dominant and undisputed factor in the various studies that have addressed the issue of estimating the parameters of a model describing the equivalent electrical circuit of a solar cell/module/panel is the criterion of performance evaluation of the used model.

According to this factor, all references have almost agreed that Relative Error (RE) is essential to evaluate the achieved results [13,16,27,37,54,55,68,69,71,73,80,84,89,90]. RE basically describes the difference between the extracted and the measured parameters in percent [94].

In order to quantify the accuracy and the goodness of the proposed models over current-voltage characteristics, a Root Mean Square Error (RMSE) analysis was also applied [16,31,33,36,37,39,42,52,53,56,60,61,66,69–71,73,77,78,84,88,95,96]. Besides, some other metrics of the magnitude of the error are possible to be used but they are not very widespread in the literature, such as the Mean Square Error (MSE) [66,91,96,97], Mean Bias Error (MBE) [16,33,39,52,56,78], Absolute Error (AE) [33,47,51,67,84,89], Individual Absolute Error (IAE) [55,71,73] and Sum of Squared Error (SSE) [13,16]. Thanks to the used performance criteria, each of these works has shown the accuracy of the problem to be solved in an efficient way. But, the difference between these different works is in the use of the experimental data to describe the real behavior of the I-V and P-V characteristic or not.

The following Tables discuss, summarize, and classify the foremost techniques for DC parameter extraction on the basis of the year of publication, the used model, the used approaches, the number of extracted DC parameters, the used data, the type of PV cells and the performance criteria. For each of the models discussed, a critical analysis of found results is carried out to highlight its advantages and disadvantages. The Tables 1–3 depict the analytical, the numerical and the metaheuristic based methodologies, respectively.

Following the critical study of published techniques related to the extraction of parameters of PV cells, Table 4 highlights the different types and models of the PV cells studied by the reviewed works.

At this stage, it is important to focus on another type of classification. Indeed, it is important to note that the use of the mathematical / analytical model is more often effective for PV cell parameter extraction if the manufacturer datasheet information's are used, whereas numerical techniques are more effective when using experimental data. The Tables 5, 6 classify the approaches methods that use datasheet information's and those that use experimental data.

As mentioned previously, the result of the issue of extraction of the parameters of a solar cell is obvious when it is followed by a serious evaluation. For this, the following section describes in detail the different evaluation criteria used in the majority of the works mentioned in the above tables (Table 1, Table 2 and Table 3) as follows:

The RMSE evaluation criterion, which compares the error between experimentally and calculated data, is defined by [16,31,33,36,39,42,52,53,60,61,66,70,78,88,93,95,96]:

$$RMSE = \sqrt{\frac{1}{N}\sum_{i=1}^{N}(I_{actual} - I_{calc})^2} \tag{77}$$

The RMSE which evaluates the objective function and used in the case of optimization problem, is given by [69,71,73,77,83,84]:

$$RMSE = \sqrt{\frac{1}{N}\sum_{i=1}^{N}(f_i(V_i, I_i, x))^2} \tag{78}$$

The equation that describes the Normalized Root Mean Square Error (NRMSE) is as follow [92]:

$$NRMSE = \frac{\sqrt{\frac{1}{N}\sum_{i=1}^{N}(I_{exp} - I_{sim})^2}}{\sqrt{\frac{1}{N}\sum_{i=1}^{N}{I_{exp}}^2}} \tag{79}$$

The Root-Mean-Square Deviation (RMSD) [93]:

$$RMSD = \sqrt{\frac{\sum_{j=1}^{N_{curve}}(I_j - I_j)^2}{N_{curve}}} \tag{80}$$

The Normalized Root-Mean-Square Deviation (NRMSD) [87,93]:

$$NRMSD(\%) = \frac{RMSD}{I_{sc}}.100 \tag{81}$$

The Mean Absolute Error (MAE) [16,64,65,69,79,84,88,96]:

$$MAE(\%) = \frac{1}{N}\sum_{i=1}^{N}|I_i - I(V_i, a)|.100 \tag{82}$$

The Mean Absolute Error in Power (MAEP) [16,93]:

$$MAEP(\%) = \frac{\sum|P_{curve} - P_{model}|}{N_{curve}}.100 \tag{83}$$

The Mean Bias Error (MBE) [16,33,39,52,56,78]:

$$MBE(\%) = \frac{1}{N}\sum_{i=1}^{N}[I_i - I(V_i, a)]^2.100 \tag{84}$$

The Mean Square Error (MSE) [66,91,96,97]:

$$MSE = \sqrt{\frac{\sum_{i=1}^{N}(I_i - i_i)^2}{N}} \tag{85}$$

The Sum Square Error (SSE) [16,56]:

$$SSE(\%) = \sum_{i=1}^{N}[I_i - I(V_i, a)]^2.100| \tag{86}$$

The value of the Residual Error of the Fitness Function (REFF) [86]:

$$REFF = \sum_{k=1}^{6} f_k^2(x) \tag{87}$$

The Absolute Error (AE) [33,47,51,67,73,78,83,84,89,97]:

Table 1
Analytical and unnamed used approaches for determining the parameters of PV cell/panel/module.

References	Year of publication	Used approaches	Number of parameters	Used data	Performance criteria	Results
[15]	2016	Mathematical techniques	Five parameters	Manufacturer I-V and P-V data	MAPE (**Eq.** 93) R^2(**Eq.** 91)	The presented discussion and classification of DC parameter extraction techniques provides a reference for researchers to select the appropriate model based on the structure of the experiment and the selected implements.
[43]	2016	Analytical and Quasi-Explicit (AQE)	Five parameters	-Real data measurements -Theoretical data	Normalized Area Error	AQE method uses just the coordinates of four arbitrary points of the I-V characteristic and their slopes. Compared with OAM method [72] and analytical five-point method [98], experimental results show that AQE exhibits fast convergence speed and high accuracy because no simplifications are used.
[62]	2016	Analytical approach	Five parameters	Measurement I-V data, R_{sh}	MAE (**Eq.** 82)	Simulation results manifest the superiority of the proposed model including the inverse dependence of the shunt resistance on the irradiance on the SDM model in terms of accuracy with the measured data and average error reduction.
[63]	2012	Analytical approach	Five parameters	Experimental I-V characteristic	-AMD -RMSd	Results shows that the model defined by the new electrical characteristics exhibits a high degree of accuracy of the operating current evaluation, even during rapid changes of solar irradiance.
[64]	2016	Unnamed	Five parameters	Standard datasets	MAE(**Eq.** 82) ACE(**eq. 100**)	Based only on good measurement of the panel temperature and the OSMP (T; VOC; ISC ; VM and IM), the proposed technique gives more accurate results, compared to other existing techniques (LMSA, CPSO, SA, PS, BMO ABSO, GA, NR). It needs simple calculation and few measurements but it is not suitable for multi-junction solar cells/panels.
[67]	2013	Analytical approach	Five parameters	Experimental I-V data from manufacturers	AE (**Eq.** 88)	The observed superior accuracy of the proposed model to describe PV modules behaviors, at any irradiance and temperature point, confirms that it allows an even better phenomenological description of the nonlinear effects of electrical mechanisms prevalent in PV modules. This might be a valuable design tool during the production as well as during the use of PV systems.
[85]	2016	Unnamed	Five parameters	Numerical informations of manufacturer data sheet	AE(**Eq.** 88)	The method simply implemented considers the error and error propagation. It provides high selective capability for users of PV module according to their requirements with more accuracy and reliability in prediction of performance of PV modules.
[86]	2015	Unnamed	Six parameters	Manufacturers' datasheet	REFF(**Eq.** 87)	This paper suggests a fast, flexible and accurate algorithm based on a reduced-form of the nonlinear system of equations for the computation of the six parameters required by the CEC6PPVMM model.
[87]	2016	Lambert W based analytical method	Five parameters	Datasheet information	NRMSD(**Eq.** 81) -CPU Execution time	The proposed method is a computational improvement of the model of De Soto, in terms of accuracy, efficiency, robustness and ease of implementation. It is very useful for various operating conditions of PV modules.
[93]	2016	Unnamed	Five parameters	Manufacturers' datasheets	MAEP(**Eq.** 83) RMSD(**Eq.** 80) NRMSD(**Eq.** 81)	● The proposed method defines a new error metric MAEP. ● It extracts the parameters using the P–V curves instead of I–V curves. ● The values ranges of estimated parameters respect their physical meaning. ● It is more accurate than well-known methods (Xiao's Method [99], Villalva's Method [100], Nonlinear Least Square (NLS) Method [101], Mahmoud's Method [102], Accarino's Method (Explicit Equations) ([103]).
[104]	2014	Theoretical analysis approach	Five parameters	Datasheet values and experimental I-V curves	-SA -AM -SD	As part of the presented theoretical and practical analysis, the developed fully mathematical approach makes it possible to simplify the procedures of the simulations of PV systems and to improve their accuracy considerably.
[105]	2017	Unnamed	Five parameters	Single I-V curve	RMSE (**Eq.** 77)	The proposed algorithm does not require the particular parameters I_{sc}, V_{oc} and P_{mmp}. It is also very important as it: ● is simple and without any approximation ● works even for incomplete I-V curves ● does not involve the slopes (dI/dV) at any point.
[110]	2013	Analytical approach	Five parameters	Datasheet values	Not mentioned	Result shows that the proposed model allows a more accurate modeling of the PV modules based solely on reference data. The model is based primarily on an analytical relationship devoid of any simplification that can affect the reliability of the results.

Table 2
Numerical used approaches for determining the parameters of PV cell/panel/module.

References	Year of publication	Used approaches	Number of parameters	Used data	Performance criteria	Results
[31]	2016	Lambert W-function based exact representat-ion (LBER)	Seven parameters	Experimental I–V, P-V data Manufacturer's I-V, P-V data	ACE (**eq.** **100**) RMSE (**Eq.** 77)	A significant result of the proposed LBER is the fact that in spite of the more time consuming, the proposed model is more accurate and robust.
[37]	2014	Analytical and numerical (Newton-Raphson) approaches	Five parameters	Experimental I-V data	RE (**Eq.** 89) NRMSE (**Eq.** 79)	The results show the superiority and validity of the application of the analytical-numerical proposed technique to merge the obtained simulated I–V curves with the experimental data.
[38]	2014	The nonlinear equation solver 'fsolve'	Five parameters	Experimental I-V and P-V curves	Derating factors	The modified simulation model was found to be valuable for accurately predicting the I-V curve characteristics of PV modules.
[39]	2015	Numerical algorithm	Five parameters	Manufacturers' I-V data	DC:r^2(**Eq.** 91) RMSE(**Eq.** 77) MBE(**Eq.** 84)	Accurate model with measured data of six crystalline silicon PV panels and acceptable suitable for practical applications
[42]	2016	Villalva [99] T. Esram [106] Vika [107]	Five parameters	Manufacturer's data sheet	RMSE(**Eq.** 77) MABE(**Eq.** 92) MAPE(**Eq.** 93)	The comparative study of Villalva [99], Esram [106] and Vika [107] algorithms performances in terms of accuracy, speed of computation, required memory space, ease of implementation and robustness, is a decision key for selecting the best extraction algorithm
[47]	2014	Lambert W function based method	Five parameters	Manufacturer datasheet	AE(**Eq.** 88)	Compared to the popular R_p model, an excellent agreement was found between the current-voltages points at the maximum point and even in case of ideality factors variations.
[54]	2011	Newton-Raphson algorithm	Four parameters	Manufacturers' I-V and P-V data	RE (**Eq.** 89)	In accordance with theoretical prediction, the accurateness of the proposed TDM based MATLAB Simulink PV system simulator reduces computational time and input parameters available on standard PV module datasheet. This has been verified for different types and large array simulation of PV modules even when interfaced with actual power electronic converters driven by MPPT algorithms.
[27]	2011	Newton- Raphson Algorithm	Four Parameters	I-V data from Manufacturers	RE (**Eq.** 89)	Thanks to its simplicity, its convergence speed and its precise correspondence with the keys points of the I-V curve, this method proves to be very effective for circuit simulators developers and photovoltaic power converters designers.
[56]	2017	Explicit Model	Eight Parameters	Experimental I-V data	SSE (**eq.** **86**)	The found results reveal that the parameter values extracted does not contradict the conventional parameters and their physical concepts.
[66]	2015	Numerical approach	Five parameters	Datasheet values provided by manufacturer-s	MSE (**Eq.** 85) RMSE (**Eq.** 77)	The presented model is able to compute accurately all the model parameters. An improvement was also reported in the Newton-Raphson's solving to accelerate the convergence.
[76]	2014	New compound method	Five parameters	Basic manufacture template data	RE(**Eq.** 89) -Prediction of the output power of real PV power stations	The proposed algorithm provides an easy, feasible and accurate mean for: ● Simulating the I–V and P–V characteristics of a PV array ● Predicting the real-time generation output of a PV power station.
[108]	2016	Runge-Kutta-Merson iterative method	Seven parameters	Datasheet I-V,P-V	Not mentioned	The computed results have been compared with different manufacturers data of U-EA110, MPV95-S, and MST-43LV modules. The outcomes of the proposed model show achieves a good improvement of the design and operation under different weather conditions.
[111]	2014	Numerical approach based on reduced forms	Five parameters	Experimental I-V curve	-Squared Error SE - RMSE (**Eq.** 77) -AE (**Eq.** 88) -MAE (**Eq.** 82) -Weighted RMSE	The presented approach allows characterizing a PV module from its measured I-V curve with an accuracy and execution time never obtained before. A comparison study with other recent and effective techniques in the forms of two different cases is established.

Table 3
Metaheuristic used approaches for determining the parameters of PV cell/panel/module.

References	Year of publication	Used approaches	Number of parameters	Used data	Performance criteria	Results
[13]	2011	Evolutionary Algorithms (EA):Genetic Algorithm (GA), Particle Swarm Optimization (PSO) and Differential Evolution (DE).	Seven parameters	Datasheet I-V data	RE(**Eq.** 89) - Fitness value -CPUtime	According to various evaluation criteria namely accuracy, consistency, speed of convergence, calculation efficiency and the number of control parameters required, it has been proved that the EA methods make it possible to construct an efficient PV system simulator and specific.
[14]	2011	PSO	Seven parameters	Experimental I-V curves	MRE (**Eq.** 90)	The PSO based parameter extraction routine can rapidly reach a good fitting of the extracted parameters of solar cells and PV modules from the I–V curves. It also seems to be a useful tool to determine the parameters that affect the performance of these devices.
[16]	2017	Shuffled Complex Evolution (SCE) technique	Seven parameters	Experiment al data	RE(**Eq.** 89) SSE(**eq.** **86**) RMSE(**Eq.** 77) MBE(**Eq.** 84) MAE(**Eq.** 82) MAEP(**Eq.** 83)	Compared with AM, LM, GA, DE, and PSO methods, the SCE presents: ● a more accuracy. ● a low convergence computational time. ● a significant ability to solve all global optimization problems.
[33]	2015	Differential Evolution with Integrated Mutation (DEIM)	Seven parameters	Experimental data and other models (PDE model [19], Rcr-IJADE [27,29,106] and IADE [109]).	-ARMSE MBE(**Eq.** 84) AE_{mppt}(**Eq.** 88) -CPU-execution time (s)	The proposed DEIM performs high accuracy and fast convergence speed. Results depict that, The average root mean square error, mean bias error, and absolute error of the proposed model at maximum power point are 1.713%, 0.149%, and 4.515%, respectively.
[36]	2016	Evolutionary Algorithms (EA): PSO CS CS-NMS GA	Five parameters Seven parameters	Experimental I-V points	-NE -RMSE (**Eq.** 77)	Referring to the good fitting of the fundamental behavior of the I–V curves, the presented approach may yield optimized solutions not as physically correct as it was expected. Thus, a correctly interpretation of the optimization results must be taken.
[50]	2014	Artificial neural Network (ANN)	Five parameters	Datasheet and experimental I-V data	Not mentioned	The ANN model can be useful to determine a higher accuracy than the conventional SDM under various operating conditions.
[51]	2011	Differential Evolution (DE)	Three parameters	Experimental I-V data from manufacturers	AE (**Eq.** 88)	The proposed model shows promising performance for any temperature and irradiance variations. It is highly effective to obtain an accurate PV module model useful for PV simulator developers.
[52]	2013	Evolutionary Algorithms (EA)	Five and seven parameters	Experimental I-V points	RMSE (**Eq.** 77) MBE (**Eq.** 84)	The electrical model using the parameters estimated by the proposed methodology showed better results than several models from literature.
[53]	2015	Simplified Bird Mating Optimizer (SBMO) approach	Five parameters	Experimental I-V data	RMSE (**Eq.** 77)	The approach (SBMO) presented is very promising in the presence of problems of optimization of photovoltaic modules.
[55]	2016	Fireworks Algorithm (FWA)	Seven parameters	I-V datasheet	IAE (**Eq.** 94) RE (**Eq.** 55)	The proposed Fireworks algorithm has been comprehensively tested with SM55 & SP70 and Kyocera200GT PV technologies. It have been also benchmarked with GA and PSO methods. The FWA algorithm allows to: ■ Reduce the probability of premature convergence. ■ Reduce computational complexity ■ Produce I-V characteristics near accurate with those of panel data sheet ■ Reduce the convergence time by 0.95s and 2.85s relative to GA and PSO, respectively. ■ Get more precision.

(*continued on next page*)

Table 3 (*continued*)

References	Year of publication	Used approaches	Number of parameters	Used data	Performance criteria	Results
[56]	2016	Differential Evolution and Electromagnetism-like algorithms	Five parameters	Experimental I-V data points	RMSE(**Eq.** 77) MBE (**Eq.** 84) CD r^2(**Eq.** 91) -CPU execution time	The found results manifest the superiority of the proposed evolutionary algorithm with integrated mutation per iteration and evolutionary algorithm with adaptive mutation per iteration, compared to electromagnetism-like algorithm. The main advantages are related to the execution time, the accuracy and the convergence.
[60]	2016	Moth-Flame optimizer (MFO) algorithm	Ten parameters	Experimental I-V characteristics	-RMSE (**Eq.** 77) -MFO -DEIM -FPA -R^2 (**Eq.** 91)	The main advantage of the MFO algorithm compared to the DEIM and FPA techniques is that it converges rapidly to optimal solutions.
[61]	2016	LMA GA DE PSO ABC	Five and seven parameters	Experimental I-V and P-V curves, current Vs time variation	RMSE (**Eq.** 77) NMAE	The ABC algorithm shows that it is very accurate, in terms of the estimated values of unknown parameters, compared to the LMA, GA, DE and PSO algorithms.
[65]	2016	Particle Swarm Optimization method	Seven parameters	Measured illuminated I-V characteristic of 82 solar cell samples	MAE(**Eq.** 82)	The suggested engineering fit model between the reverse saturation current and ideality factor of the first diode seams an easy method to predict the PV module output by reducing the number of silicon solar cell parameters needed for its modeling.
[68]	2016	Differential Evolution Technique (DET)	Five parameters Seven parameters	Experimental I-v data	IAE (**Eq.** 94) RE (**Eq.** 89) RMSE (**Eq.** 77)	Compared with ABSO, CPSO, HSA, SA, PS, OIS, and DAB parameter extraction techniques, the DET method offers more accuracy with faster convergence.
[69]	2012	Harmony Search (Hs)-based algorithms	Five and seven parameters	I-V measurement	RMSE (**Eq.** 78) RE (**Eq.** 89) MAE (**Eq.** 82)	Simulation results obtained using HS variants show that HS-based algorithms is a consistent tool for modeling PV cell systems.
[70]	2016	bio-inspiredalgorithms	Five parameters	Datasheet I-V curves	RMSE(**Eq.** 77)	The critical discussion of the different bio-inspired algorithms (GA, DE, ABC, BFA and CS) to extract the parameters of the SDM made it possible to evaluate the advantage of each algorithm in terms of the RMSE, the speed of convergence and the accuracy.
[71]	2014	Mutative-Scale Parallel Chaos OptimizationAlgorithm (MPCOA)	-Five parameters for SDM -Seven parameters for DDM	Real I-V, P-V data	RMSE(**Eq.** 78) IAE(**Eq.** 94) RE(**Eq.** 89)	The proposed MPCOA outperforms other meta-heuristic algorithms, such as GA, CPSO, ABSO, SA, PS, HSA. The proposed new technique is preferable method to determine the parameters of PV cell models.
[72]	2014	Oblique Asymptote Method (OAM)	Five parameters	Real data of voltage and current measured from a PV module	-Error between Simplified parameters A, B, C, D and E. **(Eqs.** 95–99**)** -Area between real and Estimated I-V curves.	It has been proven that OAM method is advantageous than analytical five point method. OAM approach outperforms other methods that need to know the slope of the real I-V curve near the open circuit point. Besides OAM involves a simple calculus in its resolution. OAM seems to be a useful tool to characterize PV modules and to analyze their behavior. Nevertheless, further investigations should be focused on analyzing the parameter sensitivity of this method under variation of climatic conditions.
[73]	2017	Bee pollinator Flower Pollination Algorithm (BPFPA)	-Five parameters for SDM -Seven parameters for DDM	Experimental data and other models	RMSE(**Eq.** 78) AE(**Eq.** 88) RE(**Eq.** 89) IAE(**Eq.** 94) -Curve fit accuracy -Convergence to global optimum	The proposed BPFPA method, combining ABC and FPA, was compared with Flower FPA, PS, GA, HS and ABSO algorithms. The potential in BPFPA is esteemed as it is easy to comprehend and it converges to global optimum location with fast execution speed.

(*continued on next page*)

Table 3 (*continued*)

References	Year of publication	Used approaches	Number of parameters	Used data	Performance criteria	Results
[74]	2015	Improved Free Search Differential Evolution (IFSDE)	Five parameters	Real data acquired in different temperature conditions	-Minimum, -Maximum -Median -Mean -Standard deviation of the objective function	The validity of the IFSDE is approved compared with other well-known metaheuristics, namely GA, HS and PSO. Its superiority is found particularly as it is better in escaping local optima.
[75]	2017	Particle Swarm Optimization (PSO) technique with binary constraint	Three parameters: -Ideality factor (a), -Series Resistance(R_s) -Parallel resistance (R_p)	Manufacture's data	-APE (for KD210GH-2PU) -APVE at MPP (for SP70 and SQ85)	The accuracy of the model using PSO with binary constraints is assured regardless the insolation and the temperature change. The proposed technique is also able to determine ideality factor, series and shunt resistance simultaneously without the need of estimating ideality factor and field data measurements.
[77]	2017	Modified Simplified Swarm Optimization (MSSO)	Five parameters for SDM -Seven parameters for DDM	Experimental data of 57-mm diameter commercial (R.T.C. France) silicon solar cell	RMSE(**Eq.** 77)	Compared to many other famous optimization algorithms (SSO, ABC, SBMO), the MSSO method enables better performances in terms of robustness, efficiency, accuracy and coincidence of the I-V characteristics with those of experimental data.
[78]	2015	Differential Evolution with Adaptive Mutation per iteration algorithm (DEAM)	Five parameters	Experimental data and results of other previous methods (PDE and IADE)	AE(**Eq.** 88) RMSE(**Eq.** 77) MBE(**Eq.** 84) CD-r^2(**Eq.** 91)	The improved DEAM is advantageous compared with PDE and IADE methods, in terms of accuracy, convergence, and optimal adjusted control parameters. ● Its RMSE is lower than PDE and IADE methods by about 14.3%. ● Its MBE value is less than PDE and IADE by 23.3%. The CPU-execution time is less than both PDE and IADE by 8.5% and 9% respectively.
[79]	2017	Imperialist Competitive Algorithm (ICA)	-Five parameters for SDM -Seven parameters for DDM	-Experimental data extracted from datasheets -Other reported meta-heuristic optimization algorithms	MAE(**Eq.** 82)	The proposed ICA algorithm is superior, efficient and reliable in estimating the PV cell/module optimal parameters for both SDM and DDM as it ensures the best fitness function with acceptable time.
[80]	2014	Teaching Learning Based Optimization (TLBO) algorithm	Five parameters	Experimentally measured I–V characteristics	RE(**Eq.** 89)	The proposed TLBO algorithm overcomes the limitation of various numerical methods and conventional optimization algorithms to identify the solar cell parameters. The found results exhibit that the values of extracted parameters match exactly with the reported data.
[81]	2016	Five versions of the bacterial foraging (BF) optimization algorithm	Five parameters for SDM And Seven parameters for DDM	Nameplate data of the PV module	Matching between experimental and analytical	The findings show that all various BF algorithm versions allow to reach PV module parameters. A good matching has been exhibited between experimental and analytical results with high accuracy and fast convergence speed.
[82]	2017	Based Powell's optimization method PSIM simulation model	Five parameters	Manufacturer's datasheet values measured under STC	IEC EN50530 standard	The proposed PSIM simulation model improves the accuracy by tuning the five model parameters by Powell's optimization method according to the time-varying irradiance and temperature conditions. It can be applied to various simulation programs and as the PV simulation engine in PV hardware simulators. It allows the automation of the process of extraction of the parameters which facilitates its use and guarantees uniform and very accurate results.
[83]	2016	Generalized Oppositional Teaching Learning Based Optimization (GOTLBO)	-Five parameters for SDM -Seven parameters for DDM	Experimental data	AE(**Eq.** 88) RMSE(**Eq.** 78) -ANFES -SR -Convergence graphs	The GOTLBO method uses the concept of GOBL to diminish the convergence time of original TLBO according to the initialization step and generation jumping. When compared with GA, CPSO, PS, SA, IGHS, ABSO, Rcr-IJADE and STLBO, for SDM, and with PS, SA, IGHS, ABSO, Rcr-IJADE and STLBO, for DDM, GOTLBO behaves better in terms of computational overhead and solution accuracy.

(*continued on next page*)

Table 3 (*continued*)

References	Year of publication	Used approaches	Number of parameters	Used data	Performance criteria	Results
[84]	2017	Evaporation Rate based Water Cycle Algorithm (ER-WCA)	Five parameters	Experimental data	RMSE (**Eq.** 78) AE (**Eq.** 88) MAE (**Eq.** 82) RE (**Eq.** 89) MRE (**Eq.** 90) -NFE	In terms of RMSE, MAE and MRE, the ER-WCA is advantageous to NMMPSO, GOTLBO, MABC, CSO, BBO-M methods even under changing irradiation and temperature conditions.
[88]	2017	Reduced-Space Search based method	Five parameters	Experimental I–V curves	-Number of steps -Number of Function Evaluations (FES) RMSE(**Eq.** 77) MAE(**Eq.** 82) -Solution times	This method exhibits two significant advantages: ● The ability to find high-quality solutions at a reduced computational complexity ● The possibility to be fully automated without the recourse to preliminary data selection.
[89]	2016	Genetic Algorithms (GA)	Five parameters	Manufacturers' datasheet	AE(**Eq.** 88) RE(**Eq.** 89)	● Applicability to I-V curves independently of the weather conditions. ● It does not require solving the transcendental equation describing I-V characteristic ● Satisfactory accuracy and simple calculation
[90]	2016	-LMA -TRRN -SDO	Five parameters	Measured Data	RE(**Eq.** 89) -Empirical convergence speed and model-fit accuracy	● Feasible in absence of datasheet or in case of old and degraded PV panels ● It complies with the datasheet-based method for clear sky conditions and more advantageous than it for cloudy sky conditions ● Accurate in MPP prediction.
[91]	2016	PSO-guided BF	Four parameters	Measured data	MSE(**Eq.** 85)	● PSO-guided BF could find simply the best value of the objective function and requires no mathematical derivations. ● Under different operating conditions, PSO-guided BF always exhibits least MSE.
[92]	2017	Adaptive Estimation Approach	Five parameters	Standard test conditions informations	NRMSE(**Eq.** 79)	All the results prove that the proposed method: ● Is easy to implement ● Is robust and faster than the others methods ● Is able to generate a unique and accurate solution even for impracticable initial guesses
[95]	2014	time warp invariant echo state network (TWIESN) approach	Three parameters	Real operating P-V data	RMSE(**Eq.** 77) -TIME -ERROR	Compared to the reverse propagation network (BP) model, the presented TWIESN model is more satisfactory in terms of simplicity, accuracy, robustness and efficiency regardless of the operating conditions.
[96]	2013	Artificial Neural Network (ANN)	Four and five parameter models	-Manufacturer datasheet values -Experimental testing results	CD-R^2(**Eq.** 91) MSE(**Eq.** 85) MAPE(**Eq.** 93) MAE(**Eq.** 82) -MaxabsE -MinabsE	The ANN model predicts the power and current of the PV module accurately more than the analytical models. A comparative study exhibits that the 3–7–4–1 ANN model is better than the four and five parameter models.
[97]	2016	Hybrid optimiser approach	Seven, Eight and Nine parameters	Current-voltage Experimental data	MSE(**Eq.** 85) AE(**Eq.** 88)	Results obtained using the proposed single-equation model allows fast and accurate convergence to extract the solar cells parameters even in cases of their degradation.
[112]	2015	Mean Blast Algorithm (MBA)	Five and seven parameters	Measured Values	MAE (**Eq.** 82)	The mean blast algorithm shows more efficiency and reliability compared with other competitive heuristic methods. Results highlight the matching between the measured and calculated I-V, P-V characteristics with negligible absolute errors.

(*continued on next page*)

Table 3 (*continued*)

References	Year of publication	Used approaches	Number of parameters	Used data	Performance criteria	Results
[113]	2016	Multi-verse optimization (MVO) approach	Five parameters	Experimental data and specifications by vendor's datasheets	-RMSE (**Eq.** 77) -MAE (**Eq.** 82)	It is found that the proposed MVO approach is very useful for PV power designers. It is superior to approximate mathematical method and recent heuristic-based approaches. In particular the MVO approach matches very accurately for I–V curves points with a good computational efficiency.
[114]	2015	Pattern search optimization algorithm	Five parameters	Manufacturer datasheet values	- Current error and power error in the MPP region - Extraction time	Compared to some conventional and heuristic-based optimization approaches, the developed approach shows an absolute consistency between experimental and theoretical data. The more promising thing is that these results make MVO algorithm scalable to be very useful in case of multi-diode models.
[115]	2017	Improved JAYA (IJAYA) optimization algorithm	Five and seven parameters	Experimental data	- RMSE(**Eq.** 78)	Experimental results indicate that the proposed IJAYA method is highly competitive in terms of computational overhead and solution reliability and accuracy.
[116]	2016	Adaptive Nelder-Mead simplex (NMS) hybridized with the artificial bee colony (ABC) metaheuristic algorithms, EHA-NMS	Five and seven parameters	Experimental curve	- RMSE(**Eq.** 78) - IAE(**Eq.** 94)	Experimental results compared with those of three benchmark problems of a RTC France solar cell and photowatt-PWP201 prove that the EHA-NMS outperforms other methods particularly in terms of convergence and reliability.
[117]	2017	Improved Chaotic Whale Optimization Algorithm (CWOA)	Five and seven parameters	Measured data	-RE (**Eq.** 89) -Normalized relative error -MAE (**Eq.** 82) -Normalized mean absolute error -NRMSE (**Eq.** 79) -MBE (**Eq.** 84) -Normalized mean bias error	proposed CWOA algorithm improves capabilities to extract PV cell parameter and shows high robustness and accuracy. A comparative study, supported by experimental results, with other optimization methods over different datasets is illustrated.

Table 4
Different types and models of the PV cells studied by the reviewed approaches.

References	SDM	DDM	TDM	Type of PV cells
Analytical used approaches				
[15]	✓	✓		Not mentioned
[43]	✓			Aerospace High Efficiency Silicon Cell
[62]	✓			Multi-crystalline, Mono-crystalline, CIGS, Tandem, Amorpho-us and cdte
[63]	✓			Mono-crystalline silicon
[64]	✓			35 polycrystalline panels, 32commercial mono-crystalline, 30 thin film panels.
[67]	✓			Mono-Crystalline, Multi-Crystalline and Thin-film
[85]	✓			Commercial RTC siliconsolarcells
[86]	✓			CEC6PPVMMSanyo HIT-N225A01 PV module
[87]	✓			ConergyPowerPlus 190PC, Day4 Energy 60MC-I, Perllight PLM-250P-60, Solea SM 190 and Yingli YL-165
[93]	✓			Polycrystalline PV Panel Kyocera KC200GT, Polycrystalline PV Panel Kyocera KS20T
[104]	✓			Mono-crystalline, Multi-crystalline silicon
[105]	✓			Poly-Crystalline silicon PV: PTL Solar
[110]	✓			Kyocera KC175GHT-2 and Sanyo HIT240HDE-4
Numerical used approaches				
[31]		✓		Not mentioned
[37]		✓		Not mentioned
[38]	✓			Crystalline silicon
[39]	✓			Crystalline silicon
[42]	✓			Nexpower technology (1-a-Si), NH-100UT_5A polar PV TFSMT-3x(2-*a*-Si), Xunlight XR12 (3-a-Si), First solar Fs-280 (CdTe), Sunperfect Solar CRM1753K5M-72 (mono-Si), Kyocera Solar KD210GX-LPU(Multi-Si)
[47]	✓			57 mm diameter Commercial mono-crystalline silicon cell, QCELLS mod. Q6LM cell
[54]		✓		Multi-crystalline, mono-crystalline and thin-film
[55]		✓		Multi-crystalline, Mono-crystalline and Thin-film
[56]		✓		Poly-crystalline silicon,Mono-crystalline silicon
[66]	✓			Mono-Crystalline, Poly-Crystalline, Thin-film and Amorphous
[76]	✓			Multi-crystallinePV modules (TSM-230PC05), Mono-crystalline (TSM-180DC01)
[106]		✓		Amorphous silicon and thin film
[111]	✓			Polycrystalline silicon cells Photowatt-PWP 201Silicon solar cell RTC France
Metaheuristic used approaches				
[13]		✓		Multi-crystalline, mono-crystalline and thin-film
[14]		✓		Mono-Crystalline and Multi-Crystalline silicon
[16]		✓		KC120-1 Kyocera PV module
[33]		✓		Kyocera KC120-1 multi-crystalline photovoltaic module
[36]	✓	✓		Not mentioned
[50]	✓			Multi- crystalline
[51]	✓			Multi-crystalline, mono-crystalline and thin-film
[52]	✓			Crystalline silicon and Thin film
[53]	✓			Not mentioned
[55]		✓		Mono-Crystalline and Multi-Crystalline
[56]	✓			Not mentioned
[60]			✓	Multi-crystalline silicon
[61]	✓			Crystalline silicon Amorphous silicon Micro-morph silicon
[65]		✓		Single crystalline silicon solar cells
[68]	✓	✓		Mono-Crystalline and Multi-Crystalline
[69]	✓	✓		Silicon solar cell
[70]	✓			Not mentioned
[71]	✓	✓		Multi-crystalline KC 200GTcc silicon, Mono-crystalline SQ 150-PC
[72]	✓			Polycrystalline and mono-crystalline photovoltaic modules of EURENER manufacturer
[73]	✓	✓		Kyocera KC200GT, SM55:mono-crystalline, S36: multi-crystalline, ST40: Thin Film
[74]	✓			KC200GT poly-crystalline
[75]	✓			Poly-crystalline, KD210GH-2PU, Mono-crystalline, SP70 and SQ85
[77]	✓	✓		Passivated emitter and rear cell (PERC)
[78]	✓			Multi-crystalline PV module
[79]	✓	✓		Mono-crystalline (SQ150-PC), Poly-crystalline (R.T.C France KC200GT), Amorphous(ST400)
[80]	✓			Silicon, Plastic, Dye-sensitized solar cells, Mono-crystalline si solarcell, Poly-crystalline si solar module
[81]	✓	✓		Eclipsall NRG72 PV module
[82]	✓			Crystalline Kc65gt, Kc200gt, Sq160pc
[83]	✓	✓		57 mm diameter Commercial (R.T.C. France) siliconsolarcell
[84]	✓	✓		M/s R.T.C. France pv cell, M/s photowatt (pwp-201) pv module
[88]	✓			Photowatt-PWP201 module, 57 mm diameter RTC France siliconsolarcell, aSiMicro03036-Cocoa, aSiMicro03036-Eugene, aSiMicro03038-Golden, aSiTandem72-46-Cocoa, aSiTandem72-46-Eugene, aSiTandem90-31 Golden, aSiTriple28324-Cocoa, aSiTriple28324-Eugene, aSiTriple28325-Golden, CdTe75638-Cocoa, CdTe75638-Eugene, CdTe75669-Golden, CIGS8-001-Cocoa, CIGS8-001-Eugene, CIGS1-001-Golden, CIGS39017-Cocoa, CIGS39017-Eugene, CIGS39013-Golden, HIT05667-Cocoa, HIT05667-Eugene, HIT05662-Golden, mSi0166-Cocoa, mSi0166-Eugene, mSi0247-Golden, mSi0188-Cocoa, mSi0188-Eugene, mSi0251-Golden, mSi460A8-Cocoa, mSi460A8-Eugene, mSi460BB-Golden, xSi12922-Cocoa, xSi12922-Eugene, xSi11246-Golden
[89]	✓			Polycrystalline silicon PV Panel Kyocera KC200GT
[90]	✓			300-W newly installed polycrystalline silicon panel, 210-W 20-year-old polycrystalline silicon panels
[91]	✓			LDK C1D2-140P Multi-crystalline silicon PV modules
[92]	✓			PV module KC200GT, Multi-crystalline KD201GH-2PU, Mono-crystalline Shell SQ85, Thin film Shell ST40
[95]		✓		Not mentioned
[96]	✓			Not mentioned
[97]			✓	Not mentioned

(*continued on next page*)

Table 4 (*continued*)

References	SDM	DDM	TDM	Type of PV cells
[112]	✓	✓		Poly-crystalline Si solar cell RTC France Poly-crystalline KC200GT Kyocera Multi-crystalline PW20500 Photo Watt
[113]	✓			Kyocera KC200GT RTC France Si Photowatt-PWP 201 solar module
[114]	✓			THERM Solar technik AT50, BP Solar MSX60, Kyocera KC65GT, BP Solar MSX120 Shell Solar SQ160PC, Kyocera KC200GT, Samsung LPC241SM, Trina Solar TSM245PC, and Hanwha Solar SF260
[115]	✓	✓		RTC France silicon solar cell Polycrystalline silicon cells Photowatt-PWP201
[116]	✓	✓		R.T.C France solar cell Photowatt-PWP201 PV module
[117]	✓	✓		Polycrystalline solar panel Monocrystalline solar panel

Table 5
Datasheet information based approaches.

Numerical approaches	Analytical approaches	Comments
[31] [39] [42] [47] [54] [55] [66] [76] [108]	[15] [64] [67] [85] [86] [87] [93] [104] [110]	When we ignore the deviation and abrupt variations of measurements, mathematical/analytical model can be considered as the more effective compared to the numerical solutions. For this reason, the analytical approaches are more used based on datasheet information's, which confirms that this model is only used to adjust it with the data provided by manufacturers and then to find the parameters to be determined.

Table 6
Measurement based approaches.

Numerical approaches	Analytical approaches	Comments
[31] [37] [38] [56] [111]	[43] [62] [63] [104]	Based on experimental data, it has been proven that numerical methods are more effective for determining and identifying the parameters of solar panel. This is due essentially to the research and minimization of the error between measured and extracted parameters, and that motivates those techniques compared to the analytical one.

$$AE = \mid I_{measured} - I_{calculated} \mid \tag{88}$$

The Relative Error (RE) [13,16,37,54,55,68,69,71,73,76,80,84,89,90]:

$$RE = \left| \frac{I_{measured} - I_{calculated}}{I_{measured}} \right| \tag{89}$$

The Mean Relative Error (MRE) [14,84]:

$$MRE = \frac{1}{N} \sum_{i=1}^{N} RE_i \tag{90}$$

The Coefficient of Determination (R^2) [15,39,56,60,78,96]:

$$R^2 = 1 - \frac{\sum_{i=1}^{N} (I_p - I_e)^2}{\sum_{i=1}^{N} (I_p - \frac{1}{N}\sum_{i=1}^{N} (I_e))^2} \tag{91}$$

The Mean Absolute Bias Error (MABE) [42]:

$$MABE = \frac{\sum_{i=1}^{N} (I_{estiamed} - I_{target})^2}{\sum_{i=1}^{N} (I_{estiamed} - I_{mean})^2} \tag{92}$$

The Mean Absolute Percentage Error (MAPE) [15,42,96]:

$$MAPE = \frac{1}{N} \sum_{i=1}^{N} \left| \frac{I_{estiamed} - I_{target}}{I_{target}} \right| \tag{93}$$

The Individual Absolute Error (IAE) [55,68,71,73]:

$$eIAE = |I_{t\,(measured)} - I_{t\,(calculated)}| \tag{94}$$

The Error between Simplified Parameters (ESP) A, B, C, D and E, which are given by [72]:

$$A = \frac{N_p I_{ph} R_{sh}}{R_s + R_{sh}} \tag{95}$$

$$B = \frac{N_p I_s R_{sh}}{R_s + R_{sh}} \tag{96}$$

$$C = exp\left(\frac{1}{N_s n V_t}\right) \tag{97}$$

$$D = \exp\left(\frac{R_s}{N_p n V_t}\right) \tag{98}$$

$$E = \frac{N_p}{N_s} \frac{1}{R_s + R_{sh}} \tag{99}$$

The Absolute Current Error (ACE) [31,64]:

$$ACE_{cal\_LBER} = |I_{cal\_LBER} - I| \tag{100}$$

3.3. Some directions for future researches

After reviewing, assessing and critically discussing more than 100 methods published over the past 7 years concerning the extraction of the main electric parameters of a solar cell, various issues need to be improved. The main points in concern are:

- Avoid the inaccuracy of the estimated parameters of the model by using more powerful tools in experimental measurements. In addition, a large margin of variation of the meteorological data (irradiance and temperature) must be taken into account during the measurement of the I-V characteristics. This helps particularly to better define the estimated parameters.
- Search for other effective strategies to handle the optimization problem of parameters extraction of PV cells while taking into account a more reliable comparison procedure.
- A variety of Meta heuristic optimization algorithms have already been proposed to solve the problem of identifying solar cell

parameters, such as the genetic algorithm (GA), Particle swarm PSO optimization, differential evolution (DE), Evolutionary Algorithm (EA), Artificial Neural Network (ANN), Simplified Bird Mating Optimizer (SBMO), Fireworks Algorithm (FWA), Artificial Bee Colony (ABC), Moth-Flame Optimizer (MFO) algorithm, Harmony Search (Hs) based algorithms, Mutative -Scale Parallel Chaos Optimization Algorithm (MPCOA), Differential Evolution with Integrated Mutation (DEIM), Bee Pollinator Flower Pollination Algorithm (BPFPA), Free Search Differential Evolution (FSDE), Teaching Based Learning Optimization (TLBO) algorithm, Generalized Oppositional Teaching Based Learning Optimization (GOTLBO), Evaporation Rate Based Water Cycle Algorithm (ER-WCA). In high hopes of obtaining better results than those exhibited by existing parameter identification algorithms, it is strongly recommended that the use of new algorithms or the combination of two or more algorithms together should be taken into account in future works.

- ◆ In the previous works treating Meta heuristic algorithms, each of them deals only with a single objective function by minimizing the error between the optimized parameters and those given experimentally. However, in none of the existing research, a multitude of objective functions have been compared to better choose the most appropriate parameters that describe the static characteristics of PV cells.
- ◆ In most existing works, the comparison of the error of fit has been made effectively. On the other hand, only a minority of the works were integrated the notion of execution time in their studies. For this, the CPU execution time and the convergence speed must be integrated with the other performance evaluation criteria.
- ◆ In cases where experimental data are used to extract solar cell parameters, many researchers have focused their works on a single axis in order to solve this type of problem. The comparison of a multitude of approaches that assemble analytical, numerical, and evolutionary-based algorithms in the same work seems to be unavoidable given that this contributes significantly to increase the performance of the proposed method.

4. Implementation of SDM and DDM models

4.1. I-V and P-V characteristics

From the solar cell manufacturer data sheet, we usually find five key values that are all given in the standard test condition. The parameters in question are the short circuit current I_{sc}, the open circuit voltage V_{0c}, the maximum power P_m, the temperature coefficient of the short circuit current α and the open circuit voltage β. In order to simulate a PV cell, it is crucial to first choose a suitable model that describes the equivalent electrical circuit of the latter. By selecting this model, the parameters describing the electrical circuit must be determined.

Based on the manufacturer's data sheet or experimental data, the problem of finding the different solar cell model parameters is carried out as part of searching, identifying or optimizing the parameters describing the electric circuit model. The objective is to calculate these different parameters with a minimum error and a high accuracy. This is why this type of problem has strongly attracted the researcher's attention last years.

To overcome this problem, a multitude of approaches have been proposed in the literature. These approaches can be classified into three main pillars. The first pillar is based on solving the problem by analytical methods, all of which are based on mathematical manipulations. The second one translates methodologies based on numerical approaches in the form of random algorithms. In this case, the analysis of the parameters obtained is made by a predefined tolerance, of which it describes the difference between the simulated parameters and those given by the manufacturers or experimentally. In addition, the third pillar is metaheuristic methodologies whose reformulation of the problem is declared in the form of an optimization algorithm which is based on the minimization of an objective function based on an error.

Table 7
key Specifications of different technologies of the used PV modules.

Characteristics	**Multi-crystalline BP SX 150S**	**Mono-crystalline STP270S**	**Thin-Film CHSM 5011T**
I_{sc} (A)	4.75	9.28	1.020
V_{0c} (V)	43.5	38.3	164
P_m (W)	150	270	100
I_m (A)	4.35	8.77	0.88
V_m (V)	34.5	30.8	113.6
Α	(0.065 + −0.015)%/°C	0.060%/°C	0.05%/C
Β	(−160 + −20)mV/°C	−0.34%/°C	−0.31%/C
Γ	−0.5 + −0.05%/°C	−0.41%/°C	−0.27%/C

In this review article, the most important simulations to show the difference between the extracted parameters for the SDM and the DDM models have been performed. The three different types of technologies including multi-crystalline, mono-crystalline and the thin-film have been investigated. The Table 7 depicts the key specifications of the different technologies of PV modules namely the Multi-crystalline BP SX 150S, Mono-crystalline STP270S and Thin-Film CHSM 5011T.

The current-voltage, power-voltage characteristics of the multi-crystalline BP SX 150S, mono-crystalline STP270S and thin-film CHSM 5011T models for different solar irradiance levels are respectively shown in Fig. 3, Fig. 4 and Fig. 5.

The comparison of the I-V and P-V curves derived from calculated parameters with those originate from the manufacturer for three industrial samples was performed for the SDM and DDM models using MATLAB environment. The parameters of the different models were estimated by fitting the calculated curve of the I-V and P-V characteristics to the measured I-V and P-V characteristics with an acceptable error. The calculated I-V and P-V curves of both two models for the Multi-crystalline technology are depicted by Fig. 3 illustrating the good match obtained between the two characteristics. For this technology, the variation of the solar irradiation has no influence on the characteristics obtained, except for irradiances less than 600 W/m^2 and exactly when the operating point is close to the maximum power point (MPP). In this case, the curves describing the P-V characteristics of the SDM and DDM models are not really confounded and this implies a variation around 7%.

The calculated and measured I-V and P-V curves for Mono-crystalline and Thin-film technologies for different levels of irradiance are shown in Fig. 4 and Fig. 5, respectively. For Mono-crystalline technology, the variation in solar irradiation has no influence. The I-V characteristics obtained and the three fundamentals points (I_{sc}, V_{0c} and P_m) are still within a reasonable margin for irradiance ranging from

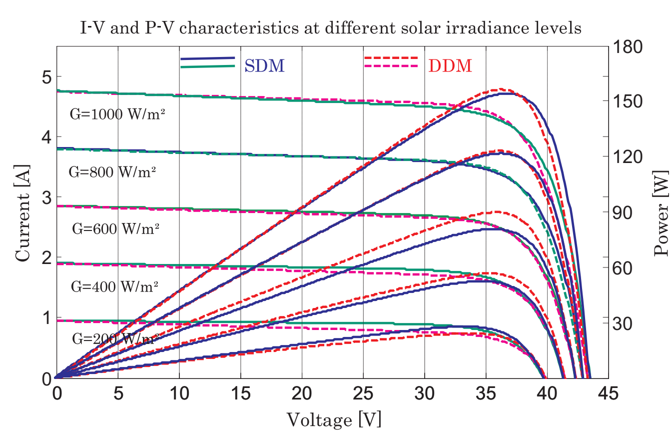

Fig. 3. I-V and P-V characteristics for different irradiation levels (**Multi-crystalline**).

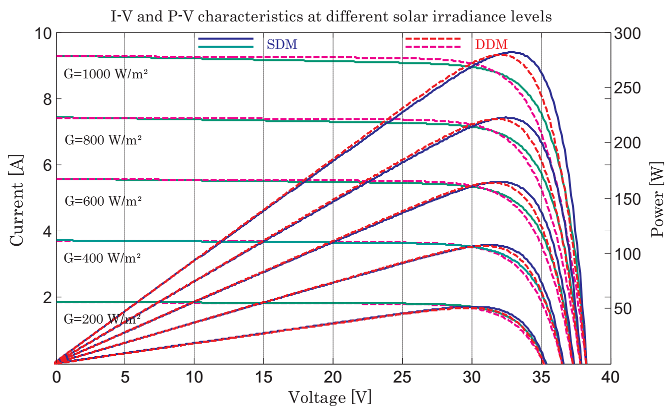

Fig. 4. I-V and P-V characteristics for different irradiation levels (**Mono-crystalline**).

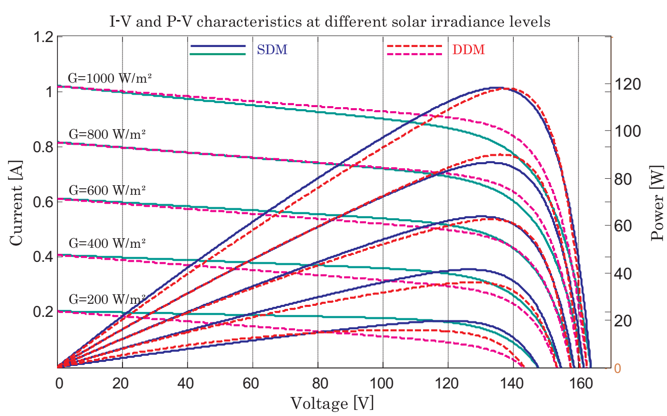

Fig. 5. I-V and P-V characteristics for different irradiation levels (**Thin-film**).

200 W/m^2 to 1000 W/m^2. In this case, the curves describing the P-V characteristics of the SDM and DDM models are not according and the error does not exceed 3%.

Regarding Thin-film technology, the I-V and P-V curves for the two studied models can seriously describe the static characteristics of the solar panel, for irradiations of 600 W/m^2, 800 W/m^2 and 1000 W/m^2. On the other hand, the difference between these two models is found in the case of irradiation levels of 200 W/m^2 and 400 W/m^2, where the current and the voltage of the maximum power point of the SDM are 5% greater than those obtained by the DDM. Besides, the same margin is almost recorded at the open circuit voltage level.

4.2. Parameters identification of PV panel

The first interesting result discussed in the Section 4.1 regards the characteristics of SDM and DDM solar cells for the three famous technologies. The Figs. 3, 4 and 5 show that it seems to be a critical for determining the five parameters of the equivalent electrical circuit of a SDM and the seven parameters of the DDM model. The various dominant extracted parameters are presented in Tables 8, 9.

For the Multi-crystalline technology, for irradiance from 1000 W/m^2 to 200 W/m^2, the shunt resistance varies from 121 Ω to 606 Ω for the SDM model and 253 Ω to 606 Ω for the DDM model. Even if the series resistance remains at a value close to 0.12 Ω for the SDM model, it varies between 0.8 Ω and 1.06 Ω for the DDM model. For both studied models, the photo-current varies from 4.75 A for an irradiation of 1000 W/m^2 up to 0.95 A for an irradiation of 200 W/m^2. Thin-Film technology is characterized by a fairly large value of shunt resistance compared to the other two technologies. In this case, the shunt

Table 8
Parameters identification of the ***SDM*** for different technologies of PV modules.

Parameters	Multi-crystalline BP SX 150S	Mono-crystalline STP270S	Thin-Film CHSM 5011T
1000 W/m^2, 25 °C			
R_{sh}	121.29	121.3	849.037
Rs	0.12	0.121	0.606
A	2.33	1.81	1.223
I0	3.44e-8	5.84e-9	8.93e-8
Isc	4.750	9.28	1.02
V0c	43.5	38.3	164
Im	4.35	8.77	0.88
Vm	36.5	33.50	128.3
Iph	4.754	9.289	1.0207
800 W/m^2, 25 °C			
R_{sh}	*151.61*	151.613	1061.296
Rs	*0.121*	0.121	0.606
A	*2.33*	1.811	1.223
I0	*3.445e-8*	5.84e-9	8.93e-8
Isc	*3.80*	7.424	0.816
VOc	*42.98*	37.895	161.72
Im	*3.48*	7.016	0.704
Vm	*36.5*	33.50	128.3
Iph	*3.80*	7.431	0.816
600 W/m^2, 25 °C			
R_{sh}	*202.15*	202.152	1415.061
Rs	*0.121*	0.121	0.6064
A	*2.33*	1.811	1.223
I0	*3.445e-8*	5.84e-9	8.93e-8
Isc	*2.85*	5.568	0.612
VOc	*42.31*	37.375	158.77
Im	*2.61*	5.262	0.528
Vm	*36.5*	33.50	128.3
Iph	*2.853*	5.573	0.612
400W/m^2, 25 °C			
R_{sh}	*303.23*	303.227	2122.59
Rs	*0.121*	0.121	0.6064
A	*2.33*	1.811	1.223
I0	*3.445e-8*	5.84e-9	8.93e-8
Isc	*1.9*	3.712	0.408
VOc	*41.36*	36.641	154.63
Im	*1.74*	3.51	0.352
Vm	*36.5*	33.50	128.3
Iph	*1.90*	3.72	0.408
200 W/m^2, 25 °C			
R_{sh}	*606.45*	606.46	*4245.18*
Rs	*0.121*	0.122	0.6064
A	*2.33*	1.811	1.223
I0	*3.44e-8*	5.84e-9	8.93e-8
Isc	*0.95*	1.856	*0.204*
VOc	*39.75*	35.385	*147.546*
Im	*0.87*	1.754	*0.176*
Vm	*36.5*	33.50	*128.3*
Iph	*0.951*	1.857	*0.204*

resistance can reach a value of 4000 Ω for an irradiance of 200 W/m^2 against 600 Ω for the SDM model and 1150 Ω for the DDM model of Mono-crystalline technology.

The Tables 8, 9 allow highlighting that the error of the values of the five and seven parameters of the SDM and DDM models, respectively, was relatively small around the points of the short circuit current and the open circuit voltage in all cases.

The recapitulation of this work proves that whatever used model is nearly appropriate to describe the behavior of the PV modules. The current-voltage and power-voltage curves of the SDM and DDM models are approximately the same for the different levels of solar irradiance. Each model has its strong and weak points. That’s why, by playing on the accuracy, the fastness (simulation time) and farther away than that on the model complexity to choose the most suitable model.

After comparison between the two different models, the obtained results indicate the durability, the accuracy and the satisfactory performance of these models to describe the real characteristics of solar panel.

Table 9
Parameters identification of the ***DDM*** for different technologies of PV modules.

Parameters	Multi-crystalline BP SX 150S	Mono-crystalline STP270S	Thin-Film CHSM 5011T
1000 W/m²*, *25 °C			
R_{sh}	253.58	925.45	1227.88
Rs	0.81	0.331	0.853
a1	1	1	1
a2	1.25	1.25	1.25
I01, I02	2.912e-10	1.504e-10	9.192e-10
Isc	4.734	9.276	0.977
V0c	43.4	38.2	163.8
Im	4.35	8.77	0.87
Vm	36.5	33.50	128.01
Iph	4.75	9.28	1.02
800 W/m², 25 °C			
R_{sh}	*260*	970.32	1361.296
Rs	*0.89*	0.36	0.85
a1	*1*	1	1
a2	*1.25*	1.25	1.25
I01, I02	2.912e-10	1.504e-10	9.192e-10
Isc	*3.878*	7.583	0.836
V0c	*42.95*	38	161.3
Im	*3.48*	7.2	0.704
Vm	36.5	33.50	128.013
Iph	*3.80*	7.424	0.816
600 W/m², 25 °C			
R_{sh}	*202.15*	990.010	1415.061
Rs	*0.951*	0.39	0.87
a1	*1*	1	1
a2	*1.25*	1.25	1.25
I01, I02	2.912e-10	1.504e-10	9.192e-10
Isc	*2.99*	5.836	0.604
V0c	*42.31*	37.15	158.77
Im	*2.61*	5.29	0.528
Vm	36.5	33.50	128.01
Iph	*2.85*	5.568	0.612
400 W/m², 25 °C			
R_{sh}	*303.23*	1013	2122.59
Rs	*1.01*	0.41	0.8
a1	*1*	1	1
a2	*1.25*	1.25	1.25
I01, I02	2.912e-10	1.504e-10	9.192e-10
Isc	*2.059*	4,01	0.405
V0c	*41.36*	36.8	154.63
Im	*1.74*	3.59	0.352
Vm	36.5	33.50	128.01
Iph	*1.9*	3.712	0.408
200 W/m², 25 °C			
R_{sh}	*606.45*	1150.41	*4245.18*
Rs	*1.06*	0.43	0.81
a1	*1*	1	1
a2	*1.25*	1.25	1.25
I01,I02	2.912e-10	1.504e-10	9.192e-10
Isc	*1.071*	2.078	0.2
V0c	*39.78*	35.20	148.9
Im	*0.92*	1.69	0.176
Vm	36.5	33.50	128.01
Iph	*0.95*	1.856	0.204

5. Conclusions

Nowadays, solar cell model parameters extraction is considered among the most attractive research topics, which largely discusses the successful exploitation of solar potential and probably renewable energy. This review article critically outlines, discusses and classifies, according to three different pillars, the main issues of the variety of published research methods on the identification of cell/panel/PV module parameters. Based on this in-depth analysis, some directions for future works have been provided to better benefit from the huge growth expected in PV systems. Indeed, although a great deal of work and effort has been done by the researchers, there is still a chance to improve some trials. Thus, the parameters that make up the equivalent electric circuit of the solar cell of which they describe the current-voltage characteristic have been restored. In this review, five and nine parameters describing respectively the SDM and the TDM were identified. The tests of these two models were made based on three different technologies that included Mono-crystalline, Multi-crystalline and Thin-Film. The authors strongly believe that this paper provides researchers, engineers and investors in the related field with an overview of the different solar cell parameters extraction methods; which would be very useful for the future.

References

[1] Geng Y, Chen W, Liu Z, Chiu ASF, Han W, Liu Z, Zhong S, Qian Y, You W, Cui X. A bibliometric review: energy consumption and greenhouse gas emissions in the residential sector. J Clean Prod 2017;159:301–16.
[2] Streimikiene D, Girdzijauskas S. Assessment of post-Kyoto climate change mitigation regimes impact on sustainable development. Renew Sustain Energy Rev 2009;77:129–41.
[3] Lau LC, Lee KT, Mohamed AR. Global warming mitigation and renewable energy policy development from the Kyoto Protocol to the Copenhagen Accord—A comment. Renew Sustain Energy Rev 2012;16:5280–4.
[4] Jha SK, Bilalovic J, Jha A, Patel N, Zhang H. Renewable energy: present research and future scope of Artificial Intelligence. Renew Sustain Energy Rev 2017;77:297–317.
[5] Abbassi R, Chebbi S. energy management strategy for a grid–connected wind-solar hybrid system with battery storage: policy for optimizing conventional energy generation. Int Rev Electr Eng 2012;7:3979–90.
[6] Abbassi A, Dami MA, Jemli M. A statistical approach for hybrid energy storage system sizing based on capacity distributions in an autonomous PV/Wind power generation system. Renew Energy 2017;103:81–93.
[7] Xu J, Li L, Zheng B. Wind energy generation technological paradigm diffusion. Renew Sustain Energy Rev 2016;59:436–49.
[8] Baghdadi F, Mohammedi K, Diaf S, Behar O. Feasibility study and energy conversion analysis of stand-alone hybrid renewable energy system. Energy Convers Manag 2015;105:471–9.
[9] Mcelroy MB, Chen X. Wind and Solar Power in the United States: status and Prospects. CSEE J Power Energy Syst 2017;3:1–6.
[10] Tsikalakis A, Tomtsi T, Hatziargyriou ND, Poullikkas A, Yasin A. Review of best practices of solar electricity resources applications in selected Middle East and North Africa (MENA) countries. Renew Sustain Energy Rev 2016;15:2838–49.
[11] Jordehi AR. Maximum power point tracking in photovoltaic (PV) systems: a review of different approaches. Renew Sustain Energy Rev 2016;65:1127–38.
[12] Herteleer B, Huyck B, Catthoor F, Driesen J, Cappelle J. Normalized efficiency of photovoltaic systems: going beyond the performance ratio. Sol Energy 2017;157:408–18.
[13] Ishaque K, Salam Z, Taheri H, Shamsudin A. A critical evaluation of EA computational methods for Photovoltaic cell parameter extraction based on two diode model. Sol Energy 2011;85:1768–79.
[14] Macabebe EQB, Sheppard CJ, Ernest, van Dyk E. Parameter extraction from I–V characteristics of PV devices. Sol Energy 2011;85:12–8.
[15] Humada AM, Hojabri M, Mekhilef S, Hamada HM. Solar cell parameters extraction based on single and double-diode models: a review. Renew Sustain Energy Rev 2016;56:494–509.
[16] Gomes RCM, Vitorino MA, Corrêa MBR, Fernandes DA, Wang R. Shuffled complex evolution on photovoltaic parameter extraction: a comparative analysis. IEEE Trans Sustain Energy 2017;8(2):805–15.
[17] Tamrakar1 R, Gupta A. A review: extraction of solar cell modeling parameter. Int J Innov Res Electr Electron Inst Control Eng 2015;3:1.
[18] Jordehi AR. Parameter estimation of solar photovoltaic (PV) cells: a review. Renew Sustain Energy Rev 2016;61:354–71.
[19] Ishaque K, Salam Z, Mekhilef S, Shamsudin A. Parameter extraction of solar photovoltaic modules using penalty-based differential evolution. Appl Energy 2012;99:297–308.
[20] Chin VJ, Salam Z, Ishaque K. Cell modelling and model parameters estimation techniques for photovoltaic simulator application: a review. Appl Energy 2015;154:500–19.
[21] Liu CC, Chen CY, Weng CY, Wang CC, Jenq FL, Cheng PJ, Wang YH, Houng MP. Physical parameters extraction from current–voltage characteristic for diodes using multiple nonlinear regression analysis. Solid-State Elect 2008;52:839–43.
[22] Lim LHI, Ye Z, Ye J, Yang D, Du H. A linear method to extract diode model parameters of solar panels from a single I-V curve. Renew Energy 2015;76:135–42.
[23] Derick M, Rani C, Rajesh M, Farrag ME, Wang Y, Busawon K. An improved optimization technique for estimation of solar photovoltaic parameters. Sol Energy 2017;157:116–24.
[24] Zhou W, Yang H, Fang Z. A novel model for photovoltaic array performance prediction. Appl Energy 2007;84(12):1187–98.
[25] Kassis A, Saad M. Analysis of multi-crystalline silicon solar cells at low illumination levels using a modified two-diode model. Sol Energy Mat Sol Cells 2010;94(12):2108–12.
[26] Khanna V, Das BK, Bisht D, Vandana, Singh PK. A three diode model for industrial solar cells and estimation of solar cell parameters using PSO algorithm. Renew Energy 2015;78:105–13.
[27] Ishaque K, Salam Z, Taheri H. Simple, fast and accurate two-diode model for

photovoltaic modules. Sol Energy Mat Sol Cells 2011;95(2):586–94.
[28] Qun N, Letian Z, Kang L. A biogeography-based optimization algorithm with mutation strategies for model parameter estimation of solar and fuel cells. Energy Convers Manag 2014;86:1173–85.
[29] Gong W, Cai Z. Parameter extraction of solar cell models using repaired adaptive differential evolution. Sol Energy 2013;94:209–20.
[30] Nassar-eddine I, Obbadi A, Errami Y, El fajri A, Agunaou M. Parameter estimation of photovoltaic modules using iterative method and the Lambert W function: a comparative study. Energy Convers Manag 2016;119:37–48.
[31] Gao X, Cui Y, Hu J, Xu G, Yu Y. Lambert W-function based exact representation for double diode model of solar cells: comparison on fitness and parameter extraction. Energy Convers Manag 2016;127:443–60.
[32] Sandrolini L, Artioli M, Reggiani U. Numerical method for the extraction of photovoltaic module double-diode model parameters through cluster analysis. Appl Energy 2010;87:442–51.
[33] Muhsen DH, Ghazali AB, Khatib T, Abed IA. Parameters extraction of double diode photovoltaic module's model based on hybrid evolutionary algorithm. Energy Convers Manag 2015;105:552–61.
[34] Et-torabi K, Nassar-eddine I, Obbadi A, Errami Y, Rmaily R, Sahnoun S, El fajri A, Agunaou M. Parameters estimation of the single and double diode photovoltaic models using a Gauss–Seidel algorithm and analytical method: a comparative study. Energy Convers Manag 2017;148:1041–54.
[35] Bana S, Saini RP. A mathematical modeling framework to evaluate the performance of single and double diode based SPV systems. Energy Rep 2016;2:171–87.
[36] Barth N, Jovanovic R, Ahzi S, Khaleel MA. PV panel single and double diode model: optimization of the parameters and temperature dependence. Sol Energy Mater Sol Cells 2016;148:87–98.
[37] Hejri M, Mokhtari H, Azizian MR, Ghandhari M, Soder L. On the Parameter extraction of a five-parameter double-diode model of photovoltaic cells and modules. IEEE J Photovolt 2014;4(3):915–23.
[38] Ma T, Yang H, Lu L. Development of a model to simulate the performance characteristics of crystalline silicon photovoltaic modules/strings/arrays. Sol Energy 2014;100:31–41.
[39] Mares O, Paulescu M, Badescu V. A simple but accurate procedure for solving the five-parameter model. Energy Convers Manag 2015;105:139–48.
[40] Mahmoud Y, Xiao W, Zeineldin HH. A simple approach to modeling and simulation of photovoltaic modules. IEEE Trans Sustain Energy 2012;3(1):185–6.
[41] Zhang Y, Gao S, Gu T. Prediction of I-V characteristics for a PV panel by combining single diode model and explicit analytical model. Sol Energy 2017;144:349–55.
[42] Ayodele TR, Ogunjuyigbe ASO, Ekoh EE. Evaluation of numerical algorithms used in extracting the parameters of a single-diode photovoltaic model. Sustain Energy Technol Assess 2016;13:51–9.
[43] Toledo FJ, Blanes JM. Analytical and quasi-explicit four arbitrary point method for extraction of solar cell single-diode model parameters. Renew Energy 2016;92:346–56.
[44] Pindado S, Cubas J. Simple mathematical approach to solar cell/panel behavior based on datasheet information. Renew Energy 2017;103:729–38.
[45] Cubas J, Pindado S, Victoria M. On the analytical approach for modeling photovoltaic systems behavior. J Power Sources 2014;247:467–74.
[46] Lineykin S, Averbukh M, Kuperman A. An improved approach to extract the single-diode equivalent circuit parameters of a photovoltaic cell/panel. Renew Sustain Energy Rev 2014;30:282–9.
[47] Peng L, Sun Y, Meng Z. An improved model and parameters extraction for photovoltaic cells using only three state points at standard test condition. J Power Sources 2014;248:621–31.
[48] Lun S, Wang S, Yang G, Guo T. A new explicit double-diode modeling method based on Lambert W-function for photovoltaic arrays. Sol Energy 2015;116:69–82.
[49] Wang G, Zhao K, Shi J, Chen W, Zhang H, Yang X, Zhao Y. An iterative approach for modeling photovoltaic modules without implicit equations. Appl Energy 2017;202:189–98.
[50] Singh KJ, Kho KLR, Singh SJ. Artificial neural network approach for more accurate solar cell electrical circuit model. Int J Comp Sci Appl (IJCSA) 2014;4:3.
[51] Ishaque K, Salam Z. An improved modeling method to determine the model parameters of photovoltaic (PV) modules using differential evolution (DE). Sol Energy 2011;85:2349–59.
[52] Siddiqui MU, Abido M. Parameter estimation for five- and seven-parameter photovoltaic electrical models using evolutionary algorithms. Appl Soft Comp 2013;13:4608–21.
[53] Askarzadeh A, Coelho LS. Determination of photovoltaic modules parameters at different operating conditions using a novel bird mating optimizer approach. Energy Convers Manag 2015;89:608–14.
[54] Ishaque K, Salam Z. Syafaruddin. A comprehensive MATLAB Simulink PV system simulator with partial shading capability based on two-diode model. Sol Energy 2011;85:2217–27.
[55] Babu TS, Ram JP, Sangeetha K, Laudani A, Rajasekar N. Parameter extraction of two diode solar PV model using Fireworks algorithm. Sol Energy 2016;140:265–76.
[56] Muhsen DH, Ghazali AB, Khatib T, Abed IA. A comparative study of evolutionary algorithms and adapting control parameters for estimating the parameters of a single-diode photovoltaic module's model. Renew Energy 2016;96:377–89.
[57] Bühler AJ, Krenzinger A. Method for photovoltaic parameter extraction according to a modified double-diode model. Prog Photovolt: Res Appl 2013;21:884–93.
[58] Khanna V, Das BK, Bisht D, Vandana, Singh PK. A three diode model for industrial solar cells and estimation of solar cell parameters using PSO algorithm. Renew Energy 2015;78:105–13.
[59] Steingrube S, Breitenstein O, Ramspeck K, Glunz S, Schenk A, Altermatt PP. Explanation of commonly observed shunt currents in c-Si solar cells by means of recombination statistics beyond the Shockley-Read-Hall approximation. J Appl Phys 2011;110:1.
[60] Allam D, Yousri DA, Eteiba MB. Parameters extraction of the three diode model for the multi-crystalline solar cell/module using Moth-Flame Optimization Algorithm. Energy Convers Manag 2016;123:535–48.
[61] Kichou S, Silvestre S, Guglielminotti L, Mora-Lopez L, Munoz-Ceron E. Comparison of two PV array models for the simulation of PV systems using five different algorithms for the parameters identification. Renew Energy 2016;99:270–9.
[62] Ruschel CS, Gasparin FP, Costa ER, Krenzinger A. Assessment of PV modules shunt resistance dependence on solar irradiance. Sol Energy 2016;133:35–43.
[63] Brano VL, Orioli A, Ciulla G. On the experimental validation of an improved five-parameter model for silicon photovoltaic modules. Sol Energy Mater Sol Cells 2012;105:27–39.
[64] Tong NT, Pora W. A parameter extraction technique exploiting intrinsic properties of solar cells. Appl Energy 2016;176:104–15.
[65] Khanna V, Das BK, Vandana, Singh PK, Sharma P, Jain SK. Statistical analysis and engineering fit models for two-diode model parameters of large area silicon solar cells. Sol Energy 2016;136:401–11.
[66] Bonkoungou D, Koalaga Z, Njomo D, Zougmore F. An improved Numerical approach for photovoltaic module parameters acquisition based on single-diode model. Int J Curr Eng Technol 2015;5(6):3735–42.
[67] Dongue SB, Njomo D, Ebengai L. An improved nonlinear five-point model for photovoltaic Modules. Hindawi Publishing Corporation. Int J Photoenergy 2013:680213.
[68] Chellaswamy C, Ramesh R. Parameter extraction of solar cell models based on adaptive differential evolution algorithm. Renew Energy 2016;97:823–37.
[69] Askarzadeh A, Rezazadeh A. Parameter identification for solar cell models using harmony search-based algorithms. Sol Energy 2012;86:3241–9.
[70] Ma J, Bi Z, Ting TO, Hao S, Hao W. Comparative performance on photovoltaic model parameter identification via bio-inspired algorithms. Sol Energy 2016;132:606–16.
[71] Yuan X, Xiang Y, He Y. Parameter extraction of solar cell models using mutative-scale parallel chaos optimization algorithm. Sol Energy 2014;108:238–51.
[72] Toledo FJ, Blanes JM. Geometric properties of the single-diode photovoltaic model and a new very simple method for parameters extraction. Renew Energy 2014;72:125–33.
[73] Ram JP, Babu TS, Dragicevic T, Rajasekar N. A new hybrid bee pollinator flower pollination algorithm for solar PV parameter estimation. Energy Convers Manag 2017;135:463–76.
[74] Ayala HVH, Coelho LS, Mariani VC, Askarzadeh A. An improved free search differential evolution algorithm: a case study on parameters identification of one diode equivalent circuit of a solar cell module. Energy 2015;93:1515–22.
[75] Bana S, Saini RP. Identification of unknown parameters of a single diode photovoltaic model using particle swarm optimization with binary constraints. Renew Energy 2017;101:1299–310.
[76] Bai J, Liu S, Hao Y, Zhang Z, Jiang M, Zhang Y. Development of a new compound method to extract the five parameters of PV modules. Energy Convers Manag 2014;79:294–303.
[77] Lin P, Cheng S, Yeh W, Chen Z, Wu L. Parameters extraction of solar cell models using a modified simplified swarm optimization algorithm. Sol Energy 2017;144:594–603.
[78] Muhsen DH, Ghazali AB, Khatib T, Abed IA. Extraction of photovoltaic module model's parameters using an improved hybrid differential evolution/electromagnetism-like algorithm. Sol Energy 2015;119:286–97.
[79] Fathy A, Rezk H. Parameter estimation of photovoltaic system using imperialist competitive algorithm. Renew Energy 2017;111:307–20.
[80] Patel SJ, Panchal AK, Kheraj V. Extraction of solar cell parameters from a single current–voltage characteristic using teaching learning based optimization algorithm. Appl Energy 2014;119:384–93.
[81] Awadallah MA. Variations of the bacterial foraging algorithm for the extraction of PV module parameters from nameplate data. Energy Convers Manag 2016;113:312–20.
[82] Park JY, Choi SJ. A novel simulation model for PV panels based on datasheet parameter tuning. Sol Energy 2017;145:90–8.
[83] Chen X, Yu K, Du W, Zhao W, Liu G. Parameters identification of solar cell models using generalized oppositional teaching learning based optimization. Energy 2016;99:170–80.
[84] Kler D, Sharma P, Banerjee A, Rana KPS, Kumar V. PV cell and module efficient parameters estimation using Evaporation Rate based Water Cycle Algorithm. Swarm Evol Comput 2017;35:93–110.
[85] Deihimi MH, Naghizadeh RA, Meyabadi AF. Systematic derivation of parameters of one exponential model for photovoltaic modules using numerical information of data sheet. Renew Energy 2016;87:676–85.
[86] Laudani A, Lozito GM, Mancilla-David F, Riganti-Fulginei F, Salvini A. An improved method for SRC parameter estimation for the CEC PV module model. Sol Energy 2015;120:525–35.
[87] Batzelis EI, Papathanassiou SA. A method for the analytical extraction of the single-diode PV model parameters. IEEE Trans Sustain Energy 2016;7(2):504–12.
[88] Cardenas AA, Carrasco M, Mancilla-David F, Street A, Cardenas R. Experimental parameter extraction in the single-diode photovoltaic model via a reduced-space search. IEEE Trans Ind Electron 2017;64(2):1468–76.
[89] Cervellini MP, Echeverría NI, Antoszczuk PD, Retegui RAG, Funes MA, González SA. Optimized parameter extraction method for photovoltaic devices model. IEEE Lat Am Trans 2016;14(4):1959–65.
[90] Bharadwaj P, Chaudhury KN, John V. Sequential optimization for PV panel

parameter estimation. IEEE J Photovolt 2016;6(5):1261–8.
[91] Awadallah MA, Venkatesh B. Bacterial foraging algorithm guided by particle swarm optimization for parameter identification of photovoltaic modules. Can J Electr Comp Eng 2016;39(2):150–7.
[92] Moshksar E, Ghanbari T. Adaptive estimation approach for parameter identification of photovoltaic modules. IEEE J Photovolt 2017;7(2):614–23.
[93] Silva EA, Bradaschia F, Cavalcanti MC, Nascimento AJ. Parameter estimation method to improve the accuracy of photovoltaic electrical model. IEEE J Photovolt 2016;6(1):278–85.
[94] Abbassi A, Gammoudi R, Dami MA, Hasnaoui O, Jemli M. An improved single-diode model parameters extraction at different operating conditions with a view to modeling a photovoltaic generator: a comparative study. Sol Energy 2017;155:478–89.
[95] Lun S, Wang S, Guo T, Du C. An I–V model based on time warp invariant echo state network for photovoltaic array with shaded solar cells. Sol Energy 2014;105:529–41.
[96] Karamirad M, Omid M, Alimardani R, Mousazadeh H, Heidari SN. ANN based simulation and experimental verification of analytical four- and five-parameters models of PV modules. Simul Model Pract Theory 2013;34:86–98.
[97] Castro FD, Laudani A, Fulginei FR, Salvini A. An in-depth analysis of the modelling of organic solar cells using multiple-diode circuits. Sol Energy 2016;135:590–7.
[98] De Blas MA, Torres JL, Prieto E, Garcia A. Selecting a suitable model for characterizing photovoltaic devices. Renew Energy 2002;25:371–80.
[99] Villalva MG, Gazoli JR, Ruppert EF. Comprehensive approach to modeling and simulation of photovoltaic arrays. IEEE Trans Power Electron 2009;24(5):1198–208.
[100] Xiao W, Dunford WG, Capel A. A novel modeling method for photovoltaic cells. In Proceedings IEEE Power Electron Spec Conference; 2004. p. 1950–1956.
[101] Nayak BK, Mohapatra A, Mohanty KB. Parameters estimation of photovoltaic module using nonlinear least square algorithm: A comparative study. In Proceedings Annu IEEE India Conference; 2013. p. 1–6.
[102] Mahmoud YK, Xiao W, Zeineldin HH. A parameterization approach for enhancing PV model accuracy. IEEE Trans Ind Electron 2013;60(12):5708–16.
[103] Accarino J, Petrone G, Ramos-Paja CA, Spagnuolo G. Symbolic algebra for the calculation of the series and parallel resistances in PV module model. In Proceedings International Conference Clean Electr Power; 2013. p. 62–66.
[104] Laudani A, Fulginei FR, Salvini A. Identification of the one-diode model for photovoltaic modules from datasheet values. Sol Energy 2014;108:432–46.
[105] Rhouma MBH, Gastli A, Ben Brahim L, Touati F, Ben Ammar M. A simple method for extracting the parameters of the PV cell single-diode model. Renew Energy 2017;113:885–94.
[106] Esram T. Modelling and control of an alternating-current photovoltaic module. in: Illinois; 2010.
[107] Vika HB. Modelling of photovoltaic modules with battery energy storage in Simulink/Matlab. Trodehim: Norwegian University of Science and Technology; 2014.
[108] Elbaset AA, Ali H, Abdelsattar M. New seven parameters model for amorphous silicon and thin film PV modules based on solar irradiance. Sol Energy 2016;138:26–35.
[109] Jiang LL, Maskell DL, Patra JC. Parameter estimation of solar cells and modulesusing an improved adaptive differential evolution algorithm. Appl Energy 2013;112:185–93.
[110] Brano VL, Ciulla G. An efficient analytical approach for obtaining a five parameters model of photovoltaic modules using only reference data. Appl Energy 2013;111:894–903.
[111] Laudani A, Fulginei FR, Salvini A. High performing extraction procedure for the one-diode model of a photovoltaic panel from experimental I–V curves by using reduced forms. Sol Energy 2014;103:316–26.
[112] El-Fergany A. Efficient tool to characterize photovoltaic generating systems using mine blast algorithm. Electr Power Compon Syst 2015;43:890–901.
[113] Ali EE, El-Hameed MA, El-Fergany AA, El-Arini MM. Parameter extraction of photovoltaic generating units using multi-verse optimizer. Sustain Energy Technol Assess 2016;17:68–76.
[114] Park J-Y, Choi S-J. A novel datasheet-based parameter extraction method for a single-diode photovoltaic array model. Sol Energy 2015;122:1235–44.
[115] Yu K, Liang JJ, Qu BY, Chen X, Wang H. Parameters identification of photovoltaic models using an improved JAYA optimization algorithm. Energy Convers Manag 2017;150:742–53.
[116] Chen Z, Wu L, Lin P, Wu Y, Cheng S. Parameters identification of photovoltaic models using hybrid adaptive Nelder-Mead simplex algorithm based on eagle strategy. Appl Energy 2016;182:47–57.
[117] Oliva D, Mohamed AEA, Hassanien AE. Parameter estimation of photovoltaic cells using an improved chaotic whale optimization algorithm. Appl Energy 2017;200:141–54.